Nanoscale

REVIEW

View Article Online
View Journal

Cite this: DOI: 10.1039/d6nr00136j

Size-dependent photophysical properties of individual halide perovskite nanocrystal quantum dots

Kenichi Cho and Yoshihiko Kanemitsu *

Lead halide perovskites are unique semiconductor materials synthesized *via* low-temperature solution methods. They are expected to play a crucial role in next-generation optoelectronics, particularly in the advancement of solar cells and light-emitting devices. Lead halide perovskite nanocrystals exhibit luminescence properties not found in conventional cadmium selenide nanocrystals, which have been the subject of the most detailed studies to date. Consequently, these new material nanocrystals show great potential for innovative light-emitting device applications. This review paper summarizes the recent works of our group at Kyoto University on the low-temperature photoluminescence spectra of single perovskite nanocrystal quantum dots, emphasizing the size-dependent optical phenomena of excitons, trions, and biexcitons.

Received 11th January 2026,
Accepted 26th February 2026

DOI: 10.1039/d6nr00136j

rsc.li/nanoscale

1. Introduction

It is a great honor and a joyous occasion to celebrate the 65th birthday of Professor Nam-Gyu Park, a towering figure and pioneer in the field of high-efficiency perovskite solar cells. To commemorate this significant milestone and recognize his profound contributions, *Nanoscale* is organizing a special collection of papers. We are particularly pleased to have contributed to the fundamental physical and chemical understanding of this new class of perovskite materials and are delighted to participate in this special review collection. This brief review summarizes the recent research achievements of the research group at Kyoto University focusing on halide perovskite nanocrystals (NCs) and discusses their intriguing properties and potential applications.

Lead halide perovskites ($APbX_3$, where A = Cs, MA (CH_3NH_3), or FA ($CH(NH_2)_2$), and X = Cl, Br, or I) have been known for a long time, with the existence of $CsPbX_3$ first reported in 1893.[1] In the 1950s, it was discovered that $CsPbX_3$ possesses a perovskite structure and is photoconductive.[2,3] In 1979, $MAPbX_3$ was synthesized using an organic methylammonium (MA) ion as the A-site cation.[4] By 2009, $MAPbI_3$ was demonstrated as a viable light-absorbing material in dye-sensitized solar cells.[5] The potential of halide perovskites as

Institute for Chemical Research, Kyoto University, Uji, Kyoto, 611-0011, Japan.
E-mail: kanemitu@scl.kyoto-u.ac.jp

Kenichi Cho

Kenichi Cho received his PhD from Kyoto University in 2024. Currently, he is working as a postdoctoral researcher at Nanoscale Quantum Photonics Laboratory, RIKEN Pioneering Research Institute. His research interests include optical properties of low-dimensional nanomaterials and quantum light source applications.

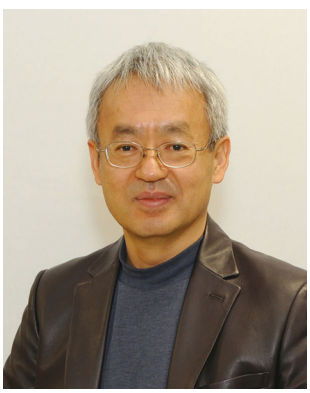

Yoshihiko Kanemitsu

Yoshihiko Kanemitsu is a Specially Appointed Professor of the Institute for Chemical Research, Kyoto University and Kyoto University Professor Emeritus. His research interests include fundamental optical and electronic properties of halide perovskites, dynamics of biexcitons and trions in nanocrystal quantum dots, and nonlinear optics of semiconductors under extremely strong electric fields.

solar cell materials are also suggested.[6] These halide perovskite materials truly entered the spotlight in 2012, when all-solid-state solar cells utilizing halide perovskites were reported with power conversion efficiencies of around 10%.[7–9] Even today, research on these materials is booming worldwide.[10–15] These ionic crystal semiconductors exhibit outstanding material properties for optoelectronic device applications; a direct bandgap structure,[16,17] defect tolerance nature,[18,19] high photoluminescence quantum yields (PLQYs),[20,21] and so on. Their material properties differ from those of conventional compound semiconductors. Our group at Kyoto University has also reported numerous achievements on halide perovskites, including: the direct bandgap determination of $MAPbI_3$ (1.61 eV),[17] band structures and polaron masses determined by nonlinear and magneto-optical spectroscopy,[22–26] recombination dynamics of free carriers and free excitons,[27–29] the photon recycling effect,[28–33] the hot phonon bottleneck effect,[34] strong coupling between phonons and vacuum photons,[35] higher harmonic generation,[36–38] the photorefractive effect,[39,40] and nonlinear optical responses in ferroelectric perovskites.[41–43] It is believed that our achievements also have contributed to elucidating the power-generation mechanisms of perovskite solar cells and to providing insights for further improving their photovoltaic efficiencies.[44,45] In addition, we have demonstrated the potential of halide perovskites for applications such as broadband light sources, optical phase modulators, and optoelectronic functional devices that integrate light emission with ferroelectricity. By employing advanced spectroscopic techniques, our research provides profound insights into the intrinsic carrier and exciton dynamics of unique halide perovskite semiconductors.

The study of NC quantum dots originated with Ekimov *et al.*, who synthesized semiconductor NCs within glasses and crystals, and successfully explained their optical properties through the quantum confinement effect.[46,47] Concurrently, Brus *et al.* explored colloidally synthesized NCs in solution, observing size-dependent optical spectra.[48,49] Following this pioneering research, the photophysical properties of semiconductor NCs, including those of CuCl,[50] CdS,[51] Ge,[52] and Si,[53–55] have been actively investigated. A significant advancement in NC quantum dot research came in 1993 with Bawendi *et al.*'s successful hot-injection synthesis of high-quality cadmium chalcogenide (CdS, CdSe, and CdTe) NCs.[56] Core-shell CdSe NCs, with precisely controllable structure and composition *via* colloidal methods,[57–59] have since become pivotal materials in NC research. Their electronic structure and photoluminescence (PL) properties have been elucidated in detail, establishing them as one of the most extensively studied material groups in nanoscience.[60] More recently, halide perovskite NCs—novel semiconductor materials exhibiting unique optical properties not found in conventional inorganic semiconductors—have emerged as the focus of intense research, leading to new developments in their photophysics.

NCs of halide perovskite exhibit superior semiconductor properties while retaining the excellent optical properties of bulk crystals. They demonstrate almost 100% PLQYs, making them particularly promising as practical luminescent materials.[61,62] Like compound semiconductor NCs such as CuCl and CdS, $CsPbX_3$ NCs were initially prepared by forming them in CsX crystal matrices, and their optical spectra were reported in the early stages of perovskite NC research.[63–65] However, few studies were conducted on these materials until the syntheses of high-quality perovskite NCs by the colloid chemistry method were reported around 2015.[66–70] As with CdSe NCs, the colloidal method, which synthesizes NCs in solutions, yields high-quality and luminescent materials. The development of a versatile solution synthesis method has enabled the production of NCs with controlled size and shape. Similarly, note that significant progress has been made in perovskite NC research. In addition to high PLQYs,[67–73] these perovskite NCs exhibit superior optical properties, such as a high radiative recombination rate at low temperatures.[74,75] These features are expected to be utilized in solar cells,[76] photodetectors,[77] light-emitting diodes (LEDs),[78,79] lasers,[80,81] and single-photon sources.[82,83] We have therefore clarified the fundamental properties of excitons, trions, and biexcitons, as well as the size dependence of exciton–phonon couplings, which are essential for these applications.[84–90]

This paper summarizes our recent advances in low-temperature PL measurements of single NCs, conducted to elucidate the optical properties of perovskite NCs. To ascertain the intrinsic properties of NCs—unaffected by size inhomogeneity and/or surrounding environment—it is crucial to perform measurements on numerous single NCs under consistent experimental conditions. Additionally, low-temperature measurements offer the benefit of sharpened PL spectra, which enables the clear observation of excitons, trions, and biexcitons,[91–93] as well as phonon sidebands arising from exciton–phonon couplings.[94,95] Through PL measurements of varying NC sizes, we have successfully determined the size dependence of fundamental properties of perovskite NCs, including trion and biexciton binding energies and exciton–phonon coupling constants. Here, we present our recent data and discuss the size dependence of the excited states of perovskite NCs.

2. Size dependence of PL peak energy

We synthesized solution-dispersed perovskite NCs of varying average sizes using the hot-injection method. $CsPbBr_3$ and $CsPbI_3$ NCs were synthesized as described in ref. 67, and $FAPbBr_3$ NCs as in ref. 70. Surface treatment was performed using ammonium thiocyanate (NH_4SCN),[96–98] and perovskite NCs exhibiting nearly 100 % PLQYs. We acquired the low-temperature PL spectra and size distributions of ensemble NC samples. Subsequently, we derived equations relating PL peak energy and size by fitting these experimental data to the formula in ref. 99, utilizing parameters listed in ref. 100–102. Fig. 1 illustrates the relationships between PL peak energy and size for $CsPbBr_3$, $FAPbBr_3$, and $CsPbI_3$ NCs at 5.5 K.[84,85,87]

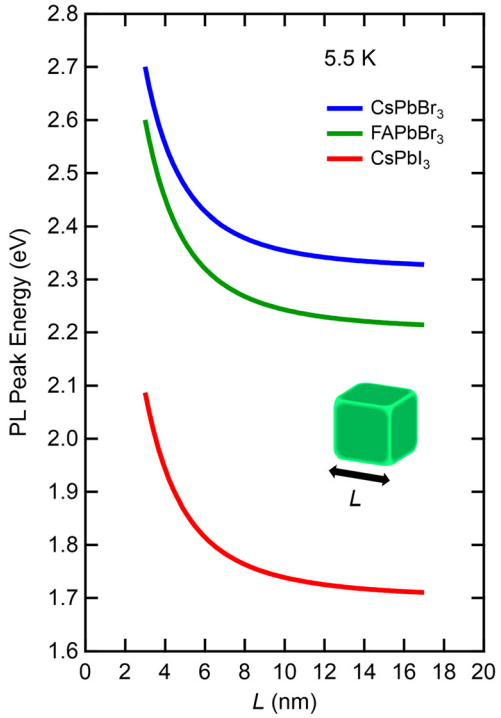

Fig. 1 PL peak energy *vs.* size for perovskite NCs of different compositions at 5.5 K. Numerical data are taken from ref. 85 for $CsPbBr_3$, ref. 84 for $FAPbBr_3$, and ref. 87 for $CsPbI_3$.

Using these relationships, we determined the NC size from the PL peak energy obtained *via* single NC spectroscopy, thereby establishing the size dependence of the PL properties of individual perovskite NCs.

3. Fine structures of PL peak

Multiple peaks are in the low-temperature PL spectra of individual perovskite NCs. Fig. 2 presents representative PL spectra from single (a) $CsPbBr_3$, (b) $CsPbI_3$, and (c) $FAPbBr_3$ NCs at 5.5 K, with peaks attributed to excitons (Ex), trions (T), and biexcitons (Bx).[87] Their identification will be detailed subsequently. The experimental methodology for all PL spectral data within this paper is thoroughly described in ref. 84–88.

First, let us discuss the exciton peak, which is the most intense peak in Fig. 2. Fig. 3(a) shows that the exciton peaks observed in single $CsPbBr_3$ NCs exhibit two or three fine structure peaks,[85] with splitting widths of approximately 1 meV.[103,104] This phenomenon occurs because triplet excitons with three energy levels are bright in $CsPbX_3$, and the orthorhombic crystal structure below room temperature allows these energy degeneracies to be resolved by the crystal field.[75,105–108] The bright triplet excitons at each of these energy levels possess transition dipoles in orthogonal directions, and the number of observed peaks depends on the orientation of the NCs relative to the detection side. Fig. 3(b) illustrates the polarization dependence of the exciton peak of a single $CsPbBr_3$ NC displaying two fine structure peaks.[85] Theoretically, the Rashba effect is predicted to raise the dark exciton level above the bright exciton level;[75,99,109] however, experimentally, PL peak from the dark exciton appears on the lower energy side of the bright exciton peak under a magnetic field.[106–108] There has been debate, both theoretical and experimental, regarding whether the lowest energy excitons are bright or dark.[75,99,106–110] In recent years, the crystal structure of halide perovskites has been revisited, and some studies have reported that they possess a polar monoclinic structure at low temperature.[111] Based on this structural model, several papers have also discussed the Rashba effect.[112] Our measurements on $CsPbBr_3$ NCs do not provide sufficient information to conclusively determine the crystal structure. How this difference in crystal symmetry influences phenomena such as exciton fine structure splitting remains an open question and will likely require further high spectral resolution measurements.

The fine structures observed in exciton peaks prove instrumental in identifying the origin of multiple peaks in perovskite NCs. As summarized in Fig. 2, the PL spectra of all-inorganic perovskite NCs are sharp, and their origins can be understood by analyzing the shapes of the peaks. Single peaks without any fine structures are trions. Since two holes have antiparallel spins to each other, no energy splitting due to electron–hole exchange interaction is observed in trion peaks. Conversely, as shown in the inset of Fig. 2, peaks with antisymmetric shapes to the exciton peaks are biexcitons, induced by biexciton–exciton cascade emission *via* the exciton fine structure levels. Other peaks, which have the same shape as the exciton peaks, are longitudinal optical (LO) phonon replicas, resulting from the coupling between excitons and LO phonons. Consequently, it is clear that trion and biexciton peaks, along with multiple LO phonon replicas (four for $CsPbBr_3$[85] and two for $FAPbBr_3$,[84] to be discussed further), are present in the low-temperature PL spectra of single perovskite NCs. The insights derived from spectral shapes align with findings from the excitation power dependence of each peak's PL intensity and the LO phonon energy shift upon halide exchange.[84] With the origin of these multiple peaks now established, a detailed discussion of perovskite NC PL properties can proceed, as outlined below.

4. Trion and biexciton binding energies

Electron–electron and exciton–exciton interactions hold significant importance for applications, as they critically impact multiexciton generation (MEG),[113–115] laser gain,[116] blinking,[117,118] and single-photon purity.[119–121] A thorough understanding of these phenomena is therefore essential for practical utility. Regarding perovskite NCs, MEG,[122,123] low-threshold amplified spontaneous emission and lasing,[124–129] and high-purity single-photon generation[130,131] have been successfully demonstrated in connection with exciton complexes. To advance our comprehension of the exciton many-body

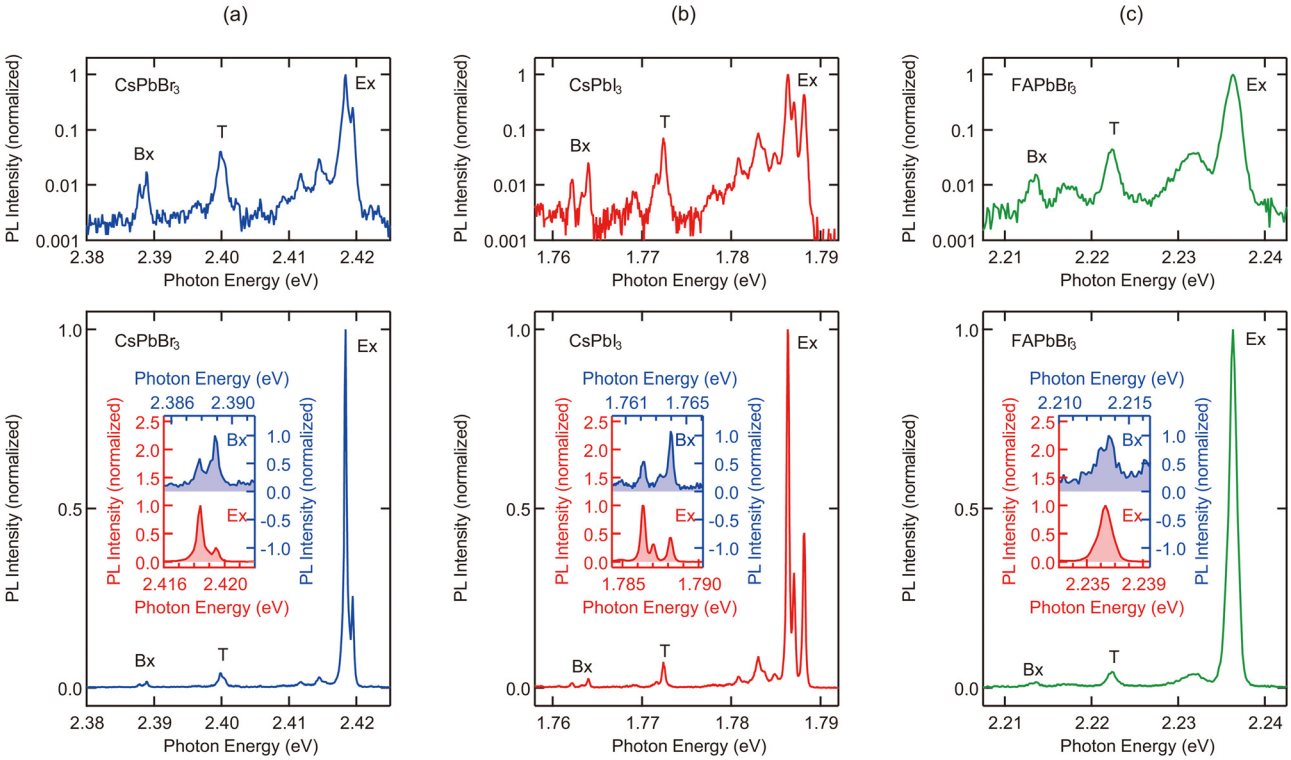

Fig. 2 Representative PL spectra of single (a) $CsPbBr_3$, (b) $CsPbI_3$, and (c) $FAPbBr_3$ NCs at 5.5 K. Upper and lower panels are shown in logarithmic and linear scales, respectively. Inset shows comparison of the fine structure splitting of the exciton (red) and biexciton (blue) peaks. Reproduced with permission from ref. 87, © American Chemical Society 2024.

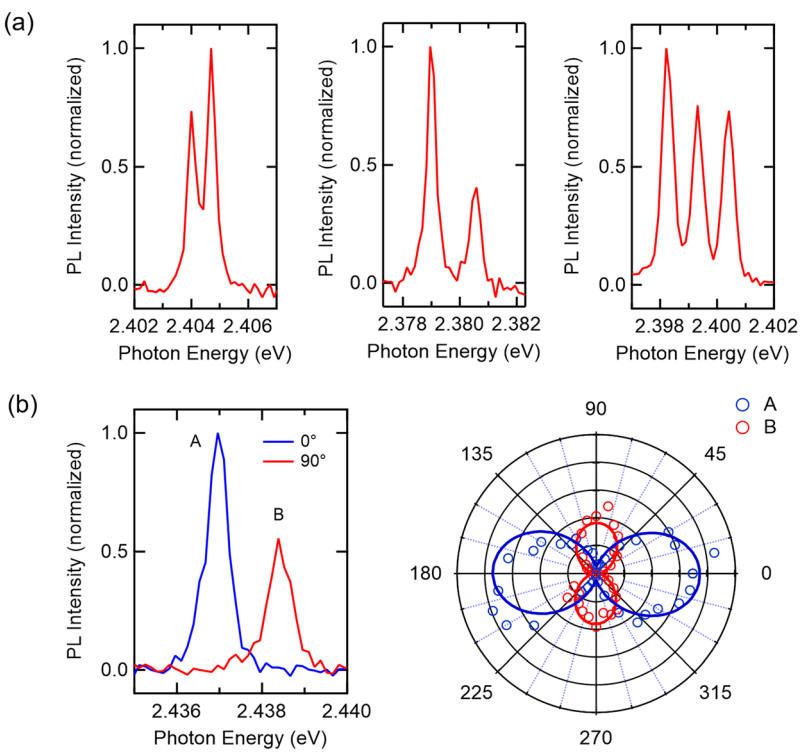

Fig. 3 (a) Two or three exciton fine structure peaks in single $CsPbBr_3$ NCs. (b) Polarization dependence of the exciton peak with two fine structure peaks. Here, the maximum PL intensity of peak A is set to 0° (180°). Reproduced with permission from ref. 85, © American Chemical Society 2022.

effects in perovskite NCs, our investigation focused on the size dependence of trion and biexciton binding energies, along with a discussion of their underlying physical mechanisms.

In addition to excitons, trions (specifically, positive trions[132]) and biexcitons are generated in perovskite NCs, where they dominate the PL spectra and dynamics.[133–135] As depicted in Fig. 2, trion and biexciton peaks become observable at low temperatures. These PL peaks appear at lower energies than exciton peaks due to their binding energies. Consequently, the size dependence of trion and biexciton binding energies can be derived from the PL spectra. While numerous studies have explored the many-body effects of excitons, measurements of binding energies in conventional nanomaterials have been scarce. Reported examples include the diameter dependence for trions in carbon nanotubes[136] and the size dependence for biexcitons in CuCl[137] and CdSe/ZnS[138] NCs. In addition, no systematic measurements have been conducted on perovskite NCs.[135] Therefore, we measured and evaluated the size dependence of trion and biexciton binding energies in perovskite NCs of different compositions ($CsPbBr_3$, $CsPbI_3$, and $FAPbBr_3$). Fig. 4 demonstrates that both trion and biexciton binding energies are independent of the A-site cations and X-site halide anions. Comparing our findings with theoretical calculations using the effective mass approximation highlights the importance of dynamic screening effects on the carrier many-body effect in perovskite NCs.

We discuss briefly the size dependence of the binding energies summarized in Fig. 4.[87] Using the elementary charge e, the Dirac constant $\hbar$, and the dielectric constant in the material ε, the bulk exciton binding energy can be defined as $\Delta_{Ex,bulk} = \frac{\mu e^4}{2\varepsilon^2\hbar^2}$ and the bulk exciton Bohr radius as $a_B = \frac{\varepsilon\hbar^2}{\mu e^2}$. We normalized the trion and biexciton binding energies by the bulk exciton binding energy, and the NC size by the bulk exciton Bohr radius. Fig. 4(a) and (b) show the normalized size dependence of the trion and biexciton binding energies, respectively. Following normalization, the data points for all compositions converge onto a single curve. This indicates that the eigenvalues of the trion and biexciton energies, when scaled by $\Delta_{Ex,bulk}$, in the many-body Hamiltonian are determined solely by the size scaled by a_B.[108] This suggests that the size dependence of the trion and biexciton binding energies of perovskite NCs follows universal scaling laws independent of composition. The binding energies exhibit minimal compositional dependence, being primarily governed by the quantum confinement effect. While theoretical discussions on binding energy size dependence have predominantly focused on $CsPbBr_3$ NCs,[139–143] this normalization method facilitates a discussion of the composition-independent, intrinsic size dependence of trion and biexciton binding energies in perovskite NCs.

To elucidate the physical properties underlying these binding energies, we conducted theoretical calculations. Nevertheless, the calculated trion and biexciton binding energies derived from the effective mass approximation were considerably smaller than our experimental observations. While dielectric screening is known to enhance binding energies,[144–149] our calculations reveal that this enhancement is insufficient to account for the experimental discrepancies. Indeed, the dielectric functions of bulk lead halide perovskites exhibit a strong dependence on the electric field frequency.[150] This substantial mismatch between experimental and theoretical results suggests that screening effects based on the static dielectric constant are inadequate. Instead, the dynamic screening effect,[151,152] which incorporates the frequency-dependent dielectric function, plays a pivotal role in perovskite NCs. Some previous studies have discussed the screening effect in the context of the polaron effect.[140–143] These compo-

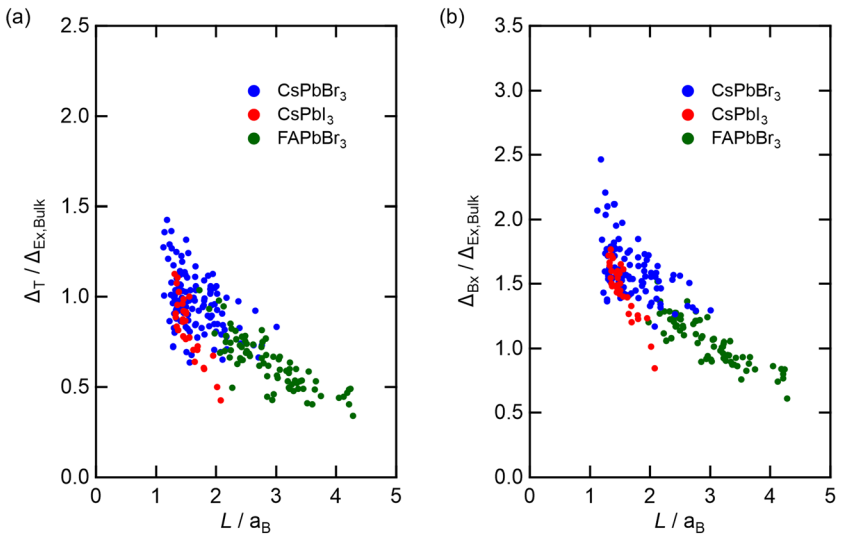

Fig. 4 Size dependence of the normalized (a) trion and (b) biexciton binding energies. Reproduced with permission from ref. 87, © American Chemical Society 2024.

sition-independent binding energies offer vital insights for comprehending carrier many-body effects in perovskites.[87]

5. Exciton–phonon couplings

Due to their ionic crystal nature, lead halide perovskites possess more flexible lattices and larger phonon–phonon and electron–phonon couplings than other semiconductor materials.[102,153] Consequently, bulk samples exhibit polarons,[25,154,155] hot phonon bottleneck effects,[34,156,157] and strong anti-Stokes PL.[158,159] Electron–phonon couplings are also significant in perovskite NCs, profoundly impacting the relaxation lifetime of hot carriers,[160–164] the efficiency of optical cooling,[165–172] and the exciton coherence time.[173–175] Therefore, a deep understanding of exciton–phonon couplings is crucial for applying perovskite NCs in solar cells, optical refrigeration, and single-photon sources. The LO phonon replicas observed in the low-temperature PL spectra of single perovskite NCs are particularly useful for studying LO phonon energies and exciton–phonon coupling strengths.

Lead halide perovskites possess extremely complex phonon structures due to their numerous constituent elements and lattice softness.[176] Many phonon sideband peaks, specifically LO phonon replicas, appear in the low-temperature PL spectra of single perovskite NCs. Fig. 5(a) displays the phonon sideband PL of excitons (LO phonon replicas) in single $CsPbBr_3$ and $FAPbBr_3$ NCs at 5.5 K.[85] In $CsPbBr_3$, four LO phonon replicas are observed, each mirroring the shape of the exciton peaks (labeled LO_1 to LO_4 from the low-energy side, respectively). Conversely, in $FAPbBr_3$, no exciton fine structure was observed; instead, only two broad LO phonon replicas were present.

To identify the origin of these LO phonon replicas, we compared them with theoretical calculations[84,85,177] and measured the energy shift of LO phonons induced by halide exchange.[84] According to the density functional theory calculations of phonon dispersions, incorporating the anharmonic approximation for bulk orthorhombic $CsPbBr_3$, LO_1 corresponds to the collective vibration of the Cs atoms in the *xy* plane and a rotation of the $PbBr_6$ octahedra. LO_2 is attributed to the $PbBr_6$ rotation. LO_3 represents the in-plane motion of the Cs and two Br atoms in the same *xy* plane. Finally, LO_4 is the stretching mode of the Pb–Br bond in the $PbBr_2$ plane. The comparison of LO phonon replicas in single $FAPbBr_3$ and $FAPbI_3$ NCs reveals shifts in LO phonon energies that are consistent with the Br/I mass ratio. Therefore, the LO phonon replicas observed in the low-temperature PL spectra of individual perovskite NCs are generated by LO phonon modes involving the PbX_6 octahedra.

Unlike all-inorganic $CsPbX_3$ NCs, $FAPbX_3$ exhibits a broad exciton peak that lacks fine structure. Additionally, its phonon sidebands are broad. The lower-energy side (phonon energy: 4.5 meV) of the two LO phonon replicas in $FAPbBr_3$ is spectrally indistinguishable from the LO phonon replicas of the phonon modes corresponding to LO_{1-3} in $CsPbBr_3$. $FAPbX_3$ NCs exhibit such broad PL spectra because the FA cation possesses a significantly larger ionic radius than the Cs cation. This stronger interaction with the PbX_6 octahedron, coupled with the presence of random dipoles arising from anisotropy,

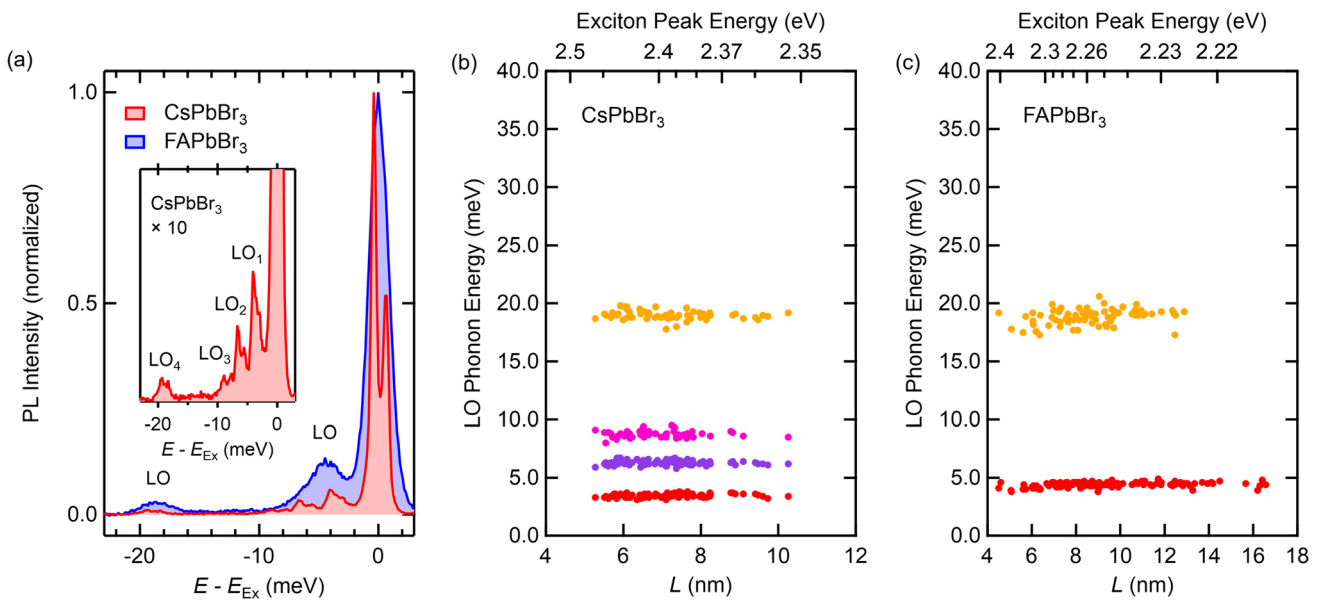

Fig. 5 (a) Comparison of LO phonon replicas of single $CsPbBr_3$ and $FAPbBr_3$ NCs; four LO phonon replicas are observed in addition to exciton fine structure in $CsPbBr_3$, while no fine structure is observed in $FAPbBr_3$ and two broad LO phonon replicas are observed. Reproduced with permission from ref. 85, © American Chemical Society 2022. (b) Size dependence of the LO phonon energies for single $CsPbBr_3$. Reproduced with permission from ref. 85, © American Chemical Society 2022. (c) Size dependence of the LO phonon energies for single $FAPbBr_3$. Reproduced with permission from ref. 84, © American Chemical Society 2021.

results in strong exciton–phonon coupling and large PL broadening compared to $CsPbBr_3$. Single $CsPbBr_3$ NCs offer the advantage of very narrow PL spectra, enabling detailed analyses of the exciton fine structure peak and the exciton–phonon coupling for each LO phonon mode.

Fig. 5(b) and (c) show the energy difference between the exciton and phonon sideband peaks for $CsPbBr_3$ and $FAPbBr_3$ NCs, respectively.[84,85] This indicates the size dependence of the LO phonon energies. However, the phonon energies themselves do not depend on size. This is likely because the optical phonon dispersion curves around the Γ point of halide perovskites are nearly flat,[178] rendering the phonon confinement effect ineffective.[54] Conversely, as illustrated in Fig. 4, both trion and biexciton binding energies become larger for smaller NCs. This is because stronger confinement leads to larger Coulomb interactions.

To discuss the exciton–phonon coupling strengths, we obtained the Huang–Rhys factors from the relative PL intensity of the LO phonon replicas to the exciton peaks. Here, we focused on $CsPbBr_3$, which exhibits narrow PL spectra, and evaluated the Huang–Rhys factors for the LO_1 and LO_2 modes. Additionally, we determined the Huang–Rhys factors for NCs with two exciton fine structure peaks. Fig. 6(a) shows these two peaks, labeled A and B, and the Huang–Rhys factors were evaluated for each peak.[85] Fig. 6(b) illustrates the dependence of the Huang–Rhys factor for peak B on exciton peak energy or size.[85] The Huang–Rhys factor increases with decreasing size. There was no significant difference between the Huang–Rhys factors for peaks A and B within the same NCs.

In general, the Huang–Rhys factor for exciton PL is greatly influenced by the spatial overlap of electron and hole wave functions. As this overlap decreases, the Huang–Rhys factor increases.[179] An internal electric field present in the NCs may be responsible for enhancing the exciton–phonon couplings.[180,181] While an internal electric field has been demonstrated in perovskite NCs through the measurement of the quantum-confined Stark effect under an electric field,[182,183] its relationship with the Huang–Rhys factor has remained unclear.

We observed the quantum-confined Stark effect by applying an electric field to single perovskite NCs and measuring the magnitude of their internal electric field.[88] Then, we examined the correlation with the Huang–Rhys factor when no external electric field was applied. Fig. 7(a) shows the response of the exciton peak of a single $CsPbBr_3$ NC when an external electric field was applied in the range of −100 to 100 kV cm^{-1}.[88] The direction of the energy shift differs for positive and negative biases, implying the presence of an internal electric field, like conventional CdSe NCs. We analyzed this energy shift in more detail. Stark shifts due to an applied external electric field generally exhibit parabolic shifts.[180,182,183] Fig. 7(b) shows the shift in exciton PL peak energy for the NC in Fig. 7(a) with respect to the applied electric field.[88] The closer the electrons and holes are to each other, the more the PL peak energy shifts toward higher energy. The electrons and holes are closest to each other at the vertex of the parabolic curve. This corresponds to the point at which the internal electric field is minimized, indicating the magnitude of the internal electric field.

Next, we examined the relationship between the internal electric field and the Huang–Rhys factor. As depicted in Fig. 7(c), the modulated internal electric field further influ-

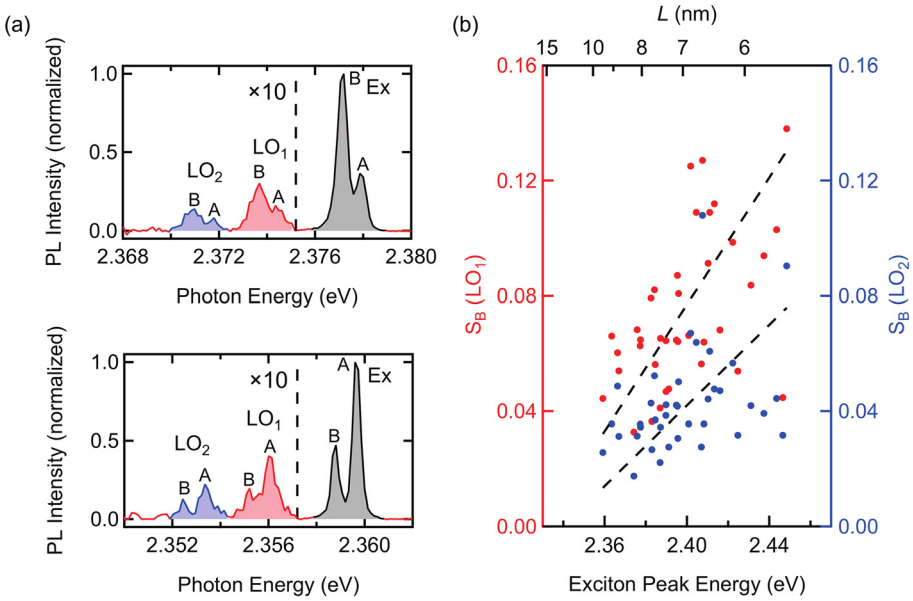

Fig. 6 (a) Exciton peaks and two LO phonon replicas (LO_1, LO_2) for single $CsPbBr_3$ NCs. The peaks are labeled A and B. (b) Exciton peak energy or size dependence of the Huang–Rhys factor in peak B ($S_B(LO_{1,2})$). The black dashed lines are the eye guides. Reproduced with permission from ref. 85, © American Chemical Society 2022.

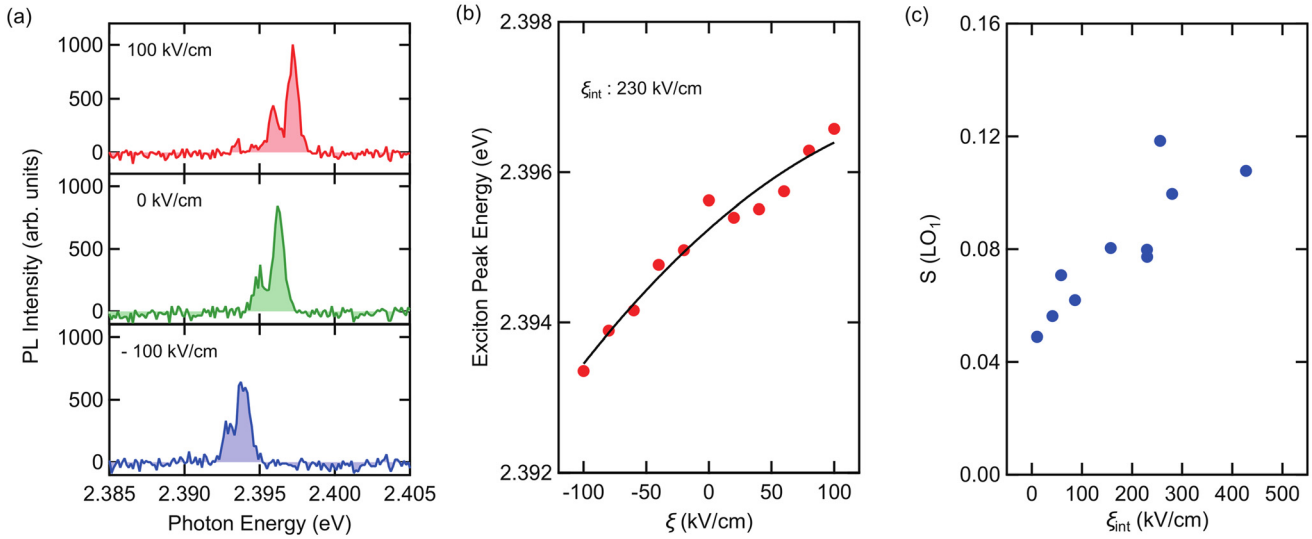

Fig. 7 (a) Exciton peak of a single $CsPbBr_3$ NC under 100 kV cm^{-1} (red), 0 kV cm^{-1} (green), and –100 kV cm^{-1} (blue) electric fields. Exciton peak energies are different for positive (100 kV cm^{-1}) and negative (–100 kV cm^{-1}) biases. (b) Dependence of the average exciton peak energy of the two peaks of the NC shown in (a) on the applied electric field (ξ). The solid line is the result of fitting by using parabolic curve. This NC shows an internal electric field (ξ_{int}) of 230 kV cm^{-1}. (c) Correlation between the internal electric field (ξ_{int}) and the Huang-Rhys factor of LO_1 at 0 kV cm^{-1} (S (LO_1)) for single $CsPbBr_3$ NCs. Reproduced with permission from ref. 88, © American Chemical Society 2024.

ences the spatial distribution of electrons and holes, consequently altering the Huang–Rhys factor.[88] We observed that the internal electric field tends to be more pronounced in smaller NCs, attributable to their larger surface-to-volume ratio. The size-dependent internal electric field can originate from two primary mechanisms: (1) Surface charges: charges located on or around the NC surface.[180,184–186] In this scenario, for smaller NCs, the reduced distance between surface charges and charge carriers (electrons and holes) may enhance their separation. (2) Lattice distortion: distortions within the NC surface lattice.[58,187] Recent studies have reported changes in Cs–Cs bond lengths near the surface of $CsPbX_3$ NCs, potentially leading to surface polarization.[188] If this lattice distortion intensifies with the size-dependent surface strain of the NCs,[189] it could account for the amplified internal electric field observed in smaller NCs. Furthermore, the significant weakening of exciton–phonon couplings in perovskite NCs with a core-shell structure provides additional support for our finding that these couplings are highly sensitive to the NC surface.[88,190] These results suggest that exciton–phonon couplings can be effectively manipulated through the application of an electric field or by modifying surface structures.[88]

6. Temperature dependence of PL spectra

Lead halide perovskites exhibit three primary crystal structures: orthorhombic, tetragonal, and cubic. These structures are temperature- and A-site cation-dependent.[191–193] A notable observation in bulk samples is a significant band gap energy shift during the orthorhombic-to-tetragonal phase transition.[22,194,195] Thus far, research on the PL properties of single perovskite NCs has mainly been performed at room temperature or liquid-helium temperatures, and there are few studies on the temperature dependence of PL properties over a wide temperature range.[196–199] Analyzing the temperature dependence of the exciton PL linewidth offers a valuable approach to investigate the impact of crystal phase transitions on exciton–phonon couplings. Furthermore, single NC spectroscopy is crucial for accurately determining the size dependence of the transition temperature and for eliminating the confounding effects of broad PL spectra caused by size inhomogeneity, which is a common issue in ensemble NC measurements.

Our study primarily investigated $FAPbBr_3$ NCs, which exhibit an orthorhombic-to-tetragonal phase transition between liquid-helium temperature and room temperature. Fig. 8(a) shows the temperature dependence of the PL spectrum of a single $FAPbBr_3$ NC up to 200 K.[86] For this NC, there is a temporal redshift of the PL spectrum around 130 K. A temporal redshift of the PL spectrum was observed around 130 K for this specific NC. To analyze these PL spectra, we performed multi-peak fitting using Gaussian or Lorentzian functions to extract the peak energies and linewidths, focusing solely on the exciton peak. Fig. 8(b) and (c) show the temperature dependence of the exciton peak energy and linewidth obtained by the fitting, respectively.[86] The solid line in Fig. 8(c) is the result of fitting using the formula in ref. 200. Although a shift in peak energy was noted around the phase transition temperature, there was no dramatic change in the linewidth. Our analysis of the temperature dependence of the PL linewidth indicates that the PL linewidth of single $FAPbBr_3$ NCs is predominantly determined by exciton–LO phonon coupling, specifi-

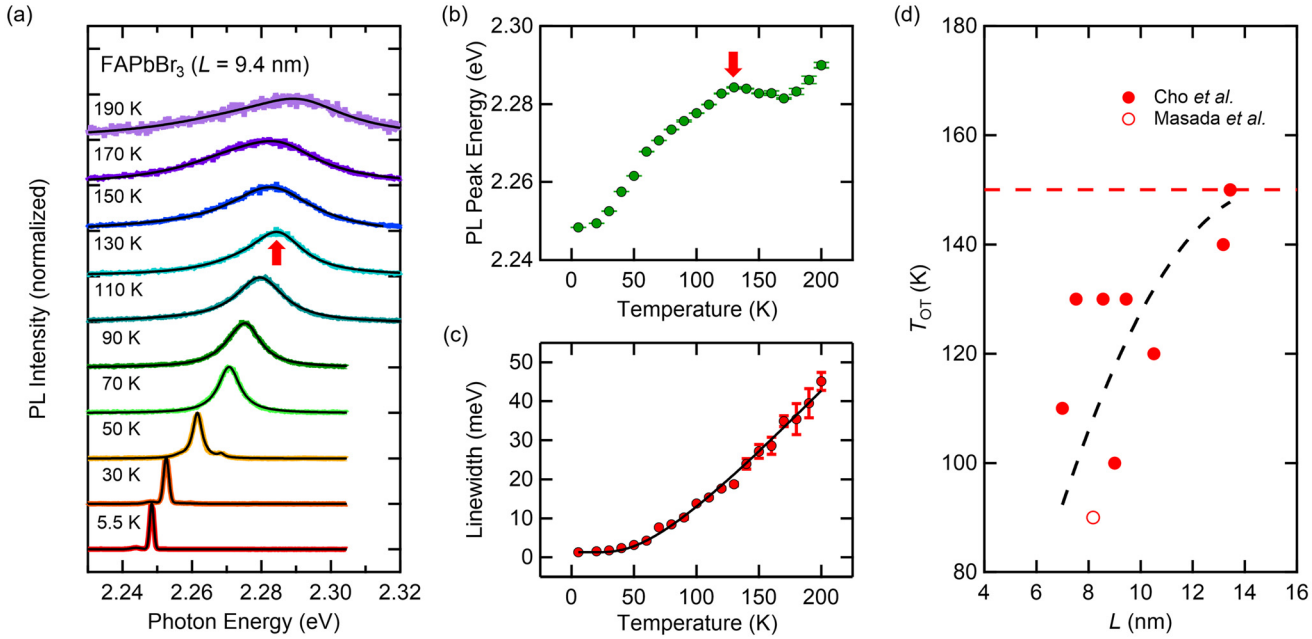

Fig. 8 (a) Temperature dependence of PL spectrum of a single $FAPbBr_3$ NC. For this NC, a redshift of the PL peak energy is observed around 130 K (red arrow), which is the phase transition from orthorhombic to tetragonal. The solid line is the fitting result, with multiple Gaussian up to 40 K and double Lorentzian above 50 K. (b) Temperature dependence of the PL peak energy of a single NC shown in (a). The error bars are sufficiently small compared to the energy shift due to the phase transition around 130–170 K. (c) Temperature dependence of PL linewidth of a single NC shown in (a). (d) Size dependence of the orthorhombic-to-tetragonal phase transition temperature (T_{OT}) of $FAPbBr_3$ NCs. Here the red circles are the data obtained in ref. 86 and the red open circle is the data obtained in ref. 199. The red dashed line is the phase transition temperature of $FAPbBr_3$ microcrystals ($L > 100$ nm). The black dashed line is the eye guide. Reproduced with permission from ref. 86, © AIP Publishing 2023.

cally the Fröhlich interaction, with an LO phonon energy of 16 meV. Importantly, this coupling appears rarely affected by the crystal phase transition. It is worth noting that $FAPbBr_3$ possesses numerous LO phonon modes; therefore, the LO phonon energy and coupling coefficients derived in this study represent effective values. These findings align well with previous studies on single crystals and thin films of materials like $MAPbX_3$,[150,201] where reported effective LO phonon energies and coupling coefficients are independent of crystal structure.

Fig. 8(d) summarizes the size dependence of the crystal phase transition temperature in single $FAPbBr_3$ NCs.[86] Here, the crystal phase transition temperature is defined as the point at which a redshift begins. As the NC size decreases, the crystal phase transition temperature also decreases. Generally, the Gibbs free energy of a crystal increases with decreasing NC size (*i.e.*, as the surface-to-volume ratio increases).[202] Consequently, the Gibbs free energy of the entire NC is inversely proportional to its size. This implies that, below a certain NC size, the tetragonal phase becomes more stable when its free energy is smaller than that of the orthorhombic phase. Like other semiconductor NCs where phase transition temperatures (such as melting point and crystal structure transition points) have been reported to decrease with decreasing size,[203,204] perovskite NCs also exhibit different crystal structures depending on their size and other factors.[76,189,205,206] Our study, utilizing single NC spectroscopy, clarifies the size dependence of the crystal phase transition temperature in these perovskite NCs.[86]

7. Conclusions

This review paper summarizes the size-dependent PL spectra of perovskite NCs, obtained *via* low-temperature single NC spectroscopy, with a focus on exciton–exciton and exciton–phonon interactions. We demonstrate that trion and biexciton binding energies and exciton–phonon couplings increase as size decreases. Additionally, we found that the crystal phase transition temperature also decreases with decreasing size. The underlying physics for this size dependence remains poorly understood, lacking quantitative discussion and requiring robust theoretical support, particularly because conventional theoretical calculations fail to capture the combined effects of strong quantum confinement, lattice softness, dynamic disorder, and surface state in perovskite NCs. A deeper understanding of exciton many-body effects and exciton–phonon couplings in perovskite NCs has been instrumental in developing: highly efficient solar cells that use MEG and hot carriers for power generation,[122,123,160–164] low-threshold lasing,[124–129] high-efficiency LEDs and high-purity single-photon generation by manipulating nonradiative Auger recombination,[130,131] optical cooling by up-conversion

PL,[165–172] and quantum light sources with high monochromaticity and long exciton coherence time.[173–175] Moreover, carrier separation induced by the internal electric field contributes to the prolongation of the spin relaxation time,[44] thereby offering potential advantages for applications in optospintronic devices.[207] In this context, quantitative theoretical frameworks that can treat Coulomb interactions and exciton–phonon couplings simultaneously are critically needed. Moreover, not only the precise control of the NC size and shape but also the manipulation of the spatial electron wavefunction profiles *via* an electric field and surface treatment is essential for tuning Coulomb interactions and exciton–phonon couplings. Therefore, elucidating the size-dependent optical phenomena of perovskite NCs is crucial for the precision design and development of the devices that leverage their unique properties. Single NC spectroscopy enabled us to elucidate the fundamental photophysical properties of perovskite NCs which are difficult to observe with ensemble NCs. Moreover, the insights obtained from single NCs can inform the understanding and design of optical properties of ensemble NCs.[208–212] For example, they will lead to an understanding of novel optical functions of superlattices of perovskite NCs and their applications.[213,214] In particular, the size dependence of exciton many-body effects and exciton–phonon couplings revealed at the single NC level are expected to serve as key design parameters for engineering collective excitonic states and emergent optical functionalities in ordered NC superlattices. Perovskite NCs, synthesized *via* the colloidal method, are highly promising materials that possess the potential to create a wide range of functionalities.

Author contributions

Kenichi Cho: visualization; writing – original draft; writing – review & editing. Yoshihiko Kanemitsu: funding acquisition; project administration; supervision; validation; writing – original draft; writing – review & editing.

Conflicts of interest

There are no conflicts to declare.

Data availability

No datasets were generated or analyzed during the current study. All relevant data are included in the cited literature.

Acknowledgements

The author would like to thank T. Yamada, H. Tahara, H. Suzuura, T. Tadano, T. Sato, M. Saruyama, R. Sato, M. Muto, H. Hirori, and T. Teranishi for the fruitful discussions. Part of this work was supported by JST CREST (JPMJCR21B4).

During the preparation of this work the authors used Google Gemini to enhance the readability and language of the manuscript. After using this tool, the authors reviewed and edited the content as needed and take full responsibility for the content of the publication.

References

1 H. L. Wells, Über die Cälsium- und Kalium-Bleihalogenide, *Z. Anorg. Chem.*, 1893, **3**, 195–210.
2 C. K. Møller, A Phase Transition in Caesium Plumbochloride, *Nature*, 1957, **180**, 981–982.
3 C. K. Møller, Crystal Structure and Photoconductivity of Caesium Plumbohalides, *Nature*, 1958, **182**, 1436.
4 D. Weber, $CH_3NH_3PbX_3$, ein Pb(II)-System mit kubischer Perowskitstruktur/$CH_3NH_3PbX_3$, a Pb(II)-System with Cubic Perovskite Structure, *Z. Naturforsch., B*, 1978, **33**, 1443–1445.
5 A. Kojima, K. Teshima, Y. Shirai and T. Miyasaka, Organometal Halide Perovskites as Visible-Light Sensitizers for Photovoltaic Cells, *J. Am. Chem. Soc.*, 2009, **131**, 6050–6051.
6 J. H. Im, C. R. Lee, J. W. Lee, S. W. Park and N.-G. Park, 6.5% efficient perovskite quantum-dot-sensitized solar cell, *Nanoscale*, 2011, **3**, 4088–4093.
7 M. M. Lee, J. Teuscher, T. Miyasaka, T. N. Murakami and H. J. Snaith, Efficient Hybrid Solar Cells Based on Meso-Superstructured Organometal Halide Perovskites, *Science*, 2012, **338**, 643–647.
8 H.-J. Kim, C.-R. Lee, J.-H. Im, K.-B. Lee, T. Moehl, A. Marchioro, S.-J. Moon, R. Humphry-Baker, J.-H. Yum, J. E. Moser, M. Grätzel and N.-G. Park, Lead Iodide Perovskite Sensitized All-Solid-State Submicron Thin Film Mesoscopic Solar Cell with Efficiency Exceeding 9%, *Sci. Rep.*, 2012, **2**, 591.
9 J. H. Heo, S. H. Im, J. H. Noh, T. N. Mandal, C.-S. Lim, J. A. Chang, Y. H. Lee, H.-J. Kim, A. Sarkar, M. K. Nazeeruddin, M. Grätzel and S. I. Seok, Efficient inorganic–organic hybrid heterojunction solar cells containing perovskite compound and polymeric hole conductors, *Nat. Photonics*, 2013, **7**, 486–491.
10 S. D. Stranks and H. J. Snaith, Metal-halide perovskites for photovoltaic and light-emitting devices, *Nat. Nanotechnol.*, 2015, **10**, 391–402.
11 L. M. Herz, Charge-Carrier Dynamics in Organic-Inorganic Metal Halide Perovskites, *Annu. Rev. Phys. Chem.*, 2016, **67**, 65–89.
12 Y. Kanemitsu, Luminescence Spectroscopy of Lead-Halide Perovskites: Materials Properties and Application as Photovoltaic Devices, *J. Mater. Chem. C*, 2017, **5**, 3427–3437.
13 Y. Kanemitsu and T. Handa, Photophysics of metal halide perovskites: From materials to devices, *Jpn. J. Appl. Phys.*, 2018, **57**, 090101.

14 L. N. Quan, B. P. Rand, R. H. Friend, S. G. Mhaisalkar, T.-W. Lee and E. H. Sargent, Perovskites for Next-Generation Optical Sources, *Chem. Rev.*, 2019, **119**, 7444–7477.
15 J. Fu, S. Ramesh, J. W. M. Lim and T. C. Sum, Carriers, Quasi-particles, and Collective Excitations in Halide Perovskites, *Chem. Rev.*, 2023, **123**, 8154–8231.
16 T. Umebayashi, K. Asai, T. Kondo and A. Nakao, Electronic structures of lead iodide based low-dimensional crystals, *Phys. Rev. B*, 2003, **67**, 155405.
17 Y. Yamada, T. Nakamura, M. Endo, A. Wakamiya and Y. Kanemitsu, Near-band-edge optical responses of solution-processed organic–inorganic hybrid perovskite $CH_3NH_3PbI_3$ on mesoporous TiO_2 electrodes, *Appl. Phys. Express*, 2014, **7**, 032302.
18 W.-J. Yin, T. Shi and Y. Yan, Unusual defect physics in $CH_3NH_3PbI_3$ perovskite solar cell absorber, *Appl. Phys. Lett.*, 2014, **104**, 063903.
19 R. E. Brandt, J. R. Poindexter, P. Gorai, R. C. Kurchin, R. L. Z. Hoye, L. Nienhaus, M. W. B. Wilson, J. A. Polizzotti, R. Sereika, R. Žaltauskas, L. C. Lee, J. L. Macmanus-Driscoll, M. Bawendi, V. Stevanović and T. Buonassisi, Searching for "Defect-Tolerant" Photovoltaic Materials: Combined Theoretical and Experimental Screening, *Chem. Mater.*, 2017, **29**, 4667–4674.
20 F. Deschler, M. Price, S. Pathak, L. E. Klintberg, D.-D. Jarausch, R. Higler, S. Hüttner, T. Leijtens, S. D. Stranks, H. J. Snaith, M. Atatüre, R. T. Phillips and R. H. Friend, High Photoluminescence Efficiency and Optically Pumped Lasing in Solution-Processed Mixed Halide Perovskite Semiconductors, *J. Phys. Chem. Lett.*, 2014, **5**, 1421–1426.
21 K. Kojima, K. Ikemura, K. Matsumori, Y. Yamada, Y. Kanemitsu and S. F. Chichibu, Internal quantum efficiency of radiation in a bulk $CH_3NH_3PbBr_3$ perovskite crystal quantified by using the omnidirectional photoluminescence spectroscopy, *APL Mater.*, 2019, **7**, 071116.
22 Y. Yamada, T. Nakamura, M. Endo, A. Wakamiya and Y. Kanemitsu, Photoelectronic Responses in Solution-Processed Perovskite $CH_3NH_3PbI_3$ Solar Cells Studied by Photoluminescence and Photoabsorption Spectroscopy, *IEEE J. Photovolt.*, 2015, **5**, 401–405.
23 K. Ohara, T. Yamada, H. Tahara, T. Aharen, H. Hirori, H. Suzuura and Y. Kanemitsu, Excitonic enhancement of optical nonlinearities in perovskite $CH_3NH_3PbCl_3$ single crystals, *Phys. Rev. Mater.*, 2019, **3**, 111601(R).
24 K. Ohara, T. Yamada, T. Aharen, H. Tahara, H. Hirori, H. Suzuura and Y. Kanemitsu, Impact of spin-orbit splitting on two-photon absorption spectra in a halide perovskite single crystal, *Phys. Rev. B*, 2021, **103**, L041201.
25 Y. Yamada, H. Mino, T. Kawahara, K. Oto, H. Suzuura and Y. Kanemitsu, Polaron Masses in $CH_3NH_3PbX_3$ Perovskites Determined by Landau Level Spectroscopy in Low Magnetic Fields, *Phys. Rev. Lett.*, 2021, **126**, 237401.
26 G. Yumoto, H. Hirori, F. Sekiguchi, R. Sato, M. Saruyama, T. Teranishi and Y. Kanemitsu, Strong spin-orbit coupling inducing Autler-Townes effect in lead halide perovskite nanocrystals, *Nat. Commun.*, 2021, **12**, 3026.
27 Y. Yamada, T. Nakamura, M. Endo, A. Wakamiya and Y. Kanemitsu, Photocarrier Recombination Dynamics in Perovskite $CH_3NH_3PbI_3$ for Solar Cell Applications, *J. Am. Chem. Soc.*, 2014, **136**, 11610–10459.
28 Y. Yamada, T. Yamada, L. Q. Phuong, N. Maruyama, H. Nishimura, A. Wakamiya, Y. Murata and Y. Kanemitsu, Dynamic Optical Properties of $CH_3NH_3PbI_3$ Single Crystals as Revealed by One- and Two-Photon Excited Photoluminescence Measurements, *J. Am. Chem. Soc.*, 2015, **137**, 10456–11613.
29 Y. Yamada, T. Yamada and Y. Kanemitsu, Free carrier radiative recombination and photon recycling in lead halide perovskite solar cell materials, *Bull. Chem. Soc. Jpn.*, 2017, **90**, 1129–1140.
30 T. Yamada, Y. Yamada, H. Nishimura, Y. Nakaike, A. Wakamiya, Y. Murata and Y. Kanemitsu, Fast Free-Carrier Diffusion in $CH_3NH_3PbBr_3$ Single Crystals Revealed by Time-Resolved One- and Two-Photon Excitation Photoluminescence Spectroscopy, *Adv. Electon. Mater.*, 2016, **2**, 1500290.
31 T. Yamada, Y. Yamada, Y. Nakaike, A. Wakamiya and Y. Kanemitsu, Photon Emission and Reabsorption Processes in $CH_3NH_3PbBr_3$ Single Crystals Revealed by Time-Resolved Two-Photon-Excitation Photoluminescence Microscopy, *Phys. Rev. Appl.*, 2017, **7**, 014001.
32 T. Yamada, T. Aharen and Y. Kanemitsu, Near-Band-Edge Optical Responses of $CH_3NH_3PbCl_3$ Single Crystals: Photon Recycling of Excitonic Luminescence, *Phys. Rev. Lett.*, 2018, **120**, 057404.
33 T. Yamada, Y. Yamada and Y. Kanemitsu, Photon recycling in perovskite $CH_3NH_3PbX_3$ (X = I, Br, Cl) bulk single crystals and polycrystalline films, *J. Lumin.*, 2020, **220**, 116987.
34 F. Sekiguchi, H. Hirori, G. Yumoto, A. Shimazaki, T. Nakamura, A. Wakamiya and Y. Kanemitsu, Enhancing the Hot-Phonon Bottleneck Effect in a Metal Halide Perovskite by Terahertz Phonon Excitation, *Phys. Rev. Lett.*, 2021, **126**, 077401.
35 Z. Zhang, H. Hirori, F. Sekiguchi, A. Shimazaki, Y. Iwasaki, T. Nakamura, A. Wakamiya and Y. Kanemitsu, Ultrastrong coupling between THz phonons and photons caused by an enhanced vacuum electric field, *Phys. Rev. Res.*, 2021, **3**, L032021.
36 H. Hirori, P. Xia, Y. Shinohara, T. Otobe, Y. Sanari, H. Tahara, N. Ishii, J. Itatani, K. L. Ishikawa, T. Aharen, M. Ozaki, A. Wakamiya and Y. Kanemitsu, High-order harmonic generation from hybrid organic–inorganic perovskite thin films, *APL Mater.*, 2019, **7**, 041107.
37 Y. Sanari, H. Hirori, T. Aharen, H. Tahara, Y. Shinohara, K. L. Ishikawa, T. Otobe, P. Xia, N. Ishii, J. Itatani, S. A. Sato and Y. Kanemitsu, Role of virtual band popu-

lation for high harmonic generation in solids, *Phys. Rev. B*, 2020, **102**, 041125(R).
38 K. Nakagawa, H. Hirori, Y. Sanari, F. Sekiguchi, R. Sato, M. Saruyama, T. Teranishi and Y. Kanemitsu, Interference effects in high-order harmonics from colloidal perovskite nanocrystals excited by an elliptically polarized laser, *Phys. Rev. Mater.*, 2021, **5**, 016001.
39 H. Tahara, T. Aharen, A. Wakamiya and Y. Kanemitsu, Photorefractive Effect in Organic–Inorganic Hybrid Perovskites and Its Application to Optical Phase Shifter, *Adv. Opt. Mater.*, 2018, **6**, 1701366.
40 T. Handa, H. Tahara, T. Aharen and Y. Kanemitsu, Large negative thermo-optic coefficients of a lead halide perovskite, *Sci. Adv.*, 2019, **5**, eaax0786.
41 T. Handa, R. Hashimoto, G. Yumoto, T. Nakamura, A. Wakamiya and Y. Kanemitsu, Metal-free ferroelectric halide perovskite exhibits visible photoluminescence correlated with local ferroelectricity, *Sci. Adv.*, 2022, **8**, eabo1621.
42 C. Higashimura, G. Yumoto, T. Yamada, T. Nakamura, F. Harata, H. Hirori, A. Wakamiya and Y. Kanemitsu, Spontaneous Polarization Induced Optical Responses in a Two-Dimensional Ferroelectric Halide Perovskite, *J. Phys. Chem. Lett.*, 2023, **14**, 8360–8366.
43 G. Yumoto, F. Harata, T. Nakamura, A. Wakamiya and Y. Kanemitsu, Electrically switchable chiral nonlinear optics in an achiral ferroelectric 2D van der Waals halide perovskite, *Sci. Adv.*, 2024, **10**, eadq5521.
44 E. Kirstein, D. R. Yakovlev, M. M. Glazov, E. Evers, E. A. Zhukov, V. V. Balykh, N. E. Kopteva, D. Kudlacik, O. Nazarenko, D. N. Dirin, M. V. Kovalenko and M. Bayer, Lead-Dominated Hyperfine Interaction Impacting the Carrier Spin Dynamics in Halide Perovskites, *Adv. Mater.*, 2022, **34**, 2105263.
45 A. L. Efros and V. G. Karpov, Electric Power and Current Collection in Semiconductor Devices with Suppressed Electron–Hole Recombination, *ACS Energy Lett.*, 2022, **7**, 3557–3563.
46 A. I. Ekimov and A. A. Onushchenko, Quantum Size Effect in Three-Dimensional Microscopic Semiconductor Crystals, *JETP Lett.*, 1981, **34**, 345–349.
47 A. I. Ekimov, A. L. Efros and A. A. Onushchenko, Quantum size effect in semiconductor microcrystals, *Solid State Commun.*, 1985, **56**, 921–924.
48 R. Rossetti, A. Nakahara and L. E. Brus, Quantum size effects in the redox potentials, resonance Raman spectra, and electronic spectra of CdS crystallites in aqueous solution, *J. Chem. Phys.*, 1983, **79**, 1086–1088.
49 L. E. Brus, Electron–electron and electron–hole interactions in small semiconductor crystallites: The size dependence of the lowest excited electronic state, *J. Chem. Phys.*, 1984, **80**, 4403–4409.
50 T. Itoh, Y. Iwabuchi and M. Kataoka, Study on the size and shape of CuCl microcrystals embedded in alkali-chloride matrices and their correlation with exciton confinement, *Phys. Status Solidi B*, 1988, **145**, 567–577.
51 Y. Wang and N. Herron, Nanometer-Sized Semiconductor Clusters: Materials Synthesis, Quantum Size Effects, and Photophysical Properties, *J. Phys. Chem.*, 1991, **25**, 525–531.
52 Y. Maeda, N. Tsukamoto, Y. Yazawa, Y. Kanemitsu and Y. Masumoto, Visible photoluminescence of Ge microcrystals embedded in SiO_2 glassy matrices, *Appl. Phys. Lett.*, 1991, **59**, 3168–3170.
53 Y. Kanemitsu, T. Ogawa, K. Shiraishi and K. Takeda, Visible photoluminescence from oxidized Si nanometer-sized spheres: Exciton confinement on a spherical shell, *Phys. Rev. B*, 1993, **48**, 4883.
54 Y. Kanemitsu, H. Uto, Y. Masumoto, T. Matsumoto, T. Futagi and H. Mimura, Microstructure and optical properties of free-standing porous silicon films: Size dependence of absorption spectra in Si nanometer-sized crystallites, *Phys. Rev. B*, 1993, **48**, 2827(R).
55 W. L. Wilson, P. F. Szajowski and L. E. Brus, Quantum confinement in size-selected, surface-oxidized silicon nanocrystals, *Science*, 1993, **262**, 1242–1244.
56 C. B. Murray, D. J. Norris and M. G. Bawendi, Synthesis and Characterization of Nearly Monodisperse CdE (E = S, Se, Te) Semiconductor Nanocrystallites, *J. Am. Chem. Soc.*, 1993, **115**, 8706–8715.
57 M. A. Hines and P. Guyot-Sionnest, Synthesis and Characterization of Strongly Luminescing ZnS-Capped CdSe Nanocrystals, *J. Phys. Chem.*, 1996, **100**, 468–471.
58 X. Peng, M. C. Schlamp, A. V. Kadavanich and A. P. Alivisatos, Epitaxial Growth of Highly Luminescent CdSe/CdS Core/Shell Nanocrystals with Photostability and Electronic Accessibility, *J. Am. Chem. Soc.*, 1997, **119**, 7019–7029.
59 B. O. Dabbousi, J. Rodoriguez-Viejo, F. V. Mikulec, J. R. Heine, H. Mattousi, R. Ober, K. F. Jensen and M. G. Bawendi, (CdSe)ZnS Core–Shell Quantum Dots: Synthesis and Characterization of a Size Series of Highly Luminescent Nanocrystallites, *J. Phys. Chem. B*, 1997, **101**, 9463–9475.
60 A. L. Efros and L. E. Brus, Nanocrystal Quantum Dots: From Discovery to Modern Development, *ACS Nano*, 2021, **15**, 6192–6210.
61 M. V. Kovalenko, L. Protesescu and M. I. Bodnarchuk, Properties and potential optoelectronic applications of lead halide perovskite nanocrystals, *Science*, 2017, **358**, 745–750.
62 Q. A. Akkerman, G. Rainò, M. V. Kovalenko and L. Manna, Genesis, challenges and opportunities for colloidal lead halide perovskite nanocrystals, *Nat. Mater.*, 2018, **17**, 394–405.
63 M. Nikl, K. Nitsch, K. Polák, G. P. Pazzi, P. Fabeni, D. S. Citrin and M. Gurioli, Optical Properties of the Pb^{2+}-based aggregated phase in a CsCl host crystal: Quantum-confinement effects, *Phys. Rev. B*, 1995, **51**, 5192–5199.
64 M. Nikl, K. Nitsch, K. Polák, E. Mihóková, S. Zazubovich, G. P. Pazzi, P. Fabeni, L. Salvini, R. Aceves, M. Barbosa-Flores, R. Perez Salas, M. Gurioli and A. Scacco, Quantum

size effect in the excitonic luminescence of $CsPbX_3$-like quantum dots in CsX (X = Cl, Br) single crystal host, *J. Lumin.*, 1997, **72**, 377–379.

65 R. Aceves, V. Babin, M. Barboza Flores, P. Fabeni, A. Maaroos, M. Nikl, K. Nitsch, G. P. Pazzi, R. Perez Salas, I. Sildos, N. Zazubovich and S. Zazubovich, Spectroscopy of $CsPbBr_3$ quantum dots in CsBr: Pb crystals, *J. Lumin.*, 2001, **93**, 27–41.

66 L. C. Schmidt, A. Pertegás, S. González-Carrero, O. Malinkiewicz, S. Agouram, G. M. Espallargas, H. J. Bolink, R. E. Galian and J. Pérez-Priento, Nontemplate Synthesis of $CH_3NH_3PbBr_3$ Perovskite Nanoparticles, *J. Am. Chem. Soc.*, 2014, **136**, 850–853.

67 L. Protesescu, S. Yakunin, M. I. Bodnarchuk, F. Krieg, R. Caputo, C. H. Hendon, R. X. Yang, A. Walsh and M. V. Kovalenko, Nanocrystals of Cesium Lead Halide Perovskites ($CsPbX_3$, X = Cl, Br, and I): Novel Optoelectronic Materials Showing Bright Emission with Wide Color Gamut, *Nano Lett.*, 2015, **15**, 3692–3696.

68 F. Zhang, H. Zhong, C. Chen, X.-G. Wu, X. Hu, H. Huang, J. Han, B. Zou and Y. Dong, Brightly Luminescent and Color-Tunable Colloidal $CH_3NH_3PbX_3$ (X=Br, I, Cl) Quantum Dots: Potential Alternatives for Display Technology, *ACS Nano*, 2015, **9**, 4533–4542.

69 O. Vybornyi, S. Yakunin and M. V. Kovalenko, Polar-solvent-free colloidal synthesis of highly luminescent alkylammonium lead halide perovskite nanocrystals, *Nanoscale*, 2016, **8**, 6278–6283.

70 L. Protesescu, S. Yakunin, M. I. Bodnarchuk, F. Bertolotti, N. Masciocchi, A. Guagliardi and M. V. Kovalenko, Monodisperse Formamidinium Lead Bromide Nanocrystals with Bright and Stable Green Photoluminescence, *J. Am. Chem. Soc.*, 2016, **138**, 14202–14205.

71 I. Levchuk, A. Osvet, X. Tang, M. Brandl, J. D. Perea, F. Hoegl, G. J. Matt, R. Hock, M. Batentschuk and C. J. Brabec, Brightly Luminescent and Color-Tunable Formamidinium Lead Halide Perovskite $FAPbX_3$ (X = Cl, Br, I) Colloidal Nanocrystals, *Nano Lett.*, 2017, **17**, 2765–2770.

72 F. Liu, Y. Zhang, C. Ding, S. Kobayashi, T. Izuishi, N. Nakazawa, T. Toyoda, T. Ohta, S. Hayase, T. Minemoto, K. Yoshino, S. Dai and Q. Shen, Highly Luminescent Phase-Stable $CsPbI_3$ Perovskite Quantum Dots Achieving Near 100% Absolute Photoluminescence Quantum Yield, *ACS Nano*, 2017, **11**, 10373–10383.

73 M. Imran, V. Caligiuri, M. Wang, L. Goldoni, M. Prato, R. Krahne, L. De Trizio and L. Manna, Benzoyl Halides as Alternative Precursors for the Colloidal Synthesis of Lead-Based Halide Perovskite Nanocrystals, *J. Am. Chem. Soc.*, 2018, **140**, 2656–2664.

74 G. Rainò, G. Nedelcu, L. Protesescu, M. I. Bodnarchuk, M. V. Kovalenko, R. F. Mahrt and T. Stöferle, Single Cesium Lead Halide Perovskite Nanocrystals at Low Temperature: Fast Single-Photon Emission, Reduced Blinking, and Exciton Fine Structure, *ACS Nano*, 2016, **10**, 2485–2490.

75 M. A. Becker, R. Vaxenberg, G. Nedelcu, P. C. Sercel, A. Shabaev, M. J. Mehl, J. G. Michopoulos, S. G. Lambrakos, N. Bernstein, J. L. Lyons, T. Stöferle, R. F. Mahrt, M. V. Kovalenko, D. J. Norris, G. Rainò and A. L. Efros, Bright triplet excitons in caesium lead halide perovskites, *Nature*, 2018, **553**, 189–193.

76 A. Swarnkar, A. R. Marshall, E. M. Sanehira, B. D. Chernomordik, D. T. Moore, J. A. Christians, T. Chakrabarti and J. M. Luther, Quantum dot–induced phase stabilization of α-$CsPbI_3$ perovskite for high-efficiency photovoltaics, *Science*, 2016, **354**, 92–95.

77 P. Ramasamy, D.-H. Lim, B. Kim, S.-H. Lee, M.-S. Lee and J.-S. Lee, All-inorganic cesium lead halide perovskite nanocrystals for photodetector applications, *Chem. Commun.*, 2016, **52**, 2067–2070.

78 J. Song, J. Li, X. Li, L. Xu, Y. Dong and H. Zeng, Quantum Dot Light-Emitting Diodes Based on Inorganic Perovskite Cesium Lead Halides ($CsPbX_3$), *Adv. Mater.*, 2015, **27**, 7162–7167.

79 A. Swarnkar, R. Chulliyil, V. K. Ravi, M. Irfanullah, A. Chowdhury and A. Nag, Colloidal $CsPbBr_3$ Perovskite Nanocrystals: Luminescence beyond Traditional Quantum Dots, *Angew. Chem., Int. Ed.*, 2015, **54**, 15424–15428.

80 S. Yakunin, L. Protesescu, F. Krieg, M. I. Bodnarchuk, G. Nedelcu, M. Humer, G. De Luca, M. Fiebig, W. Heiss and M. V. Kovalenko, Low-threshold amplified spontaneous emission and lasing from colloidal nanocrystals of caesium lead halide perovskites, *Nat. Commun.*, 2015, **6**, 8056.

81 Y. Wang, X. Li, J. Song, L. Xiao, X. Zeng and H. Sun, All-Inorganic Colloidal Perovskite Quantum Dots: A New Class of Lasing Materials with Favorable Characteristics, *Adv. Mater.*, 2015, **27**, 7101–7108.

82 Y.-S. Park, S. Guo, N. S. Makarov and V. I. Klimov, Room Temperature Single-Photon Emission from Individual Perovskite Quantum Dots, *ACS Nano*, 2015, **9**, 10386–10393.

83 F. Hu, H. Zhang, C. Sun, C. Yin, B. Lv, C. Zhang, W. W. Yu, X. Wang, Y. Zhang and M. Xiao, Superior Optical Properties of Perovskite Nanocrystals as Single Photon Emitters, *ACS Nano*, 2015, **9**, 12410–12416.

84 K. Cho, T. Yamada, H. Tahara, T. Tadano, H. Suzuura, M. Saruyama, R. Sato, T. Teranishi and Y. Kanemitsu, Luminescence Fine Structures in Single Lead Halide Perovskite Nanocrystals: Size Dependence of the Exciton–Phonon Coupling, *Nano Lett.*, 2021, **21**, 7206–7212.

85 K. Cho, H. Tahara, T. Yamada, H. Suzuura, T. Tadano, R. Sato, M. Saruyama, H. Hirori, T. Teranishi and Y. Kanemitsu, Exciton–Phonon and Trion–Phonon Couplings Revealed by Photoluminescence Spectroscopy of Single $CsPbBr_3$ Perovskite Nanocrystals, *Nano Lett.*, 2022, **22**, 7674–7681.

86 K. Cho, T. Yamada, M. Saruyama, R. Sato, T. Teranishi and Y. Kanemitsu, Temperature dependence of photoluminescence spectrum of single lead halide perovskite nanocrystals: Effect of size on the phase transition temperature, *J. Chem. Phys.*, 2023, **158**, 201104.

87 K. Cho, T. Sato, T. Yamada, R. Sato, M. Saruyama, T. Teranishi, H. Suzuura and Y. Kanemitsu, Size Dependence of Trion and Biexciton Binding Energies in Lead Halide Perovskite Nanocrystals, *ACS Nano*, 2024, **18**, 5723–5729.

88 K. Cho, H. Tahara, T. Yamada, M. Muto, M. Saruyama, R. Sato, T. Teranishi and Y. Kanemitsu, Internal Electric Field Manipulates Exciton–Phonon Couplings in Single Lead Halide Perovskite Nanocrystals, *J. Phys. Chem. Lett.*, 2024, **15**, 11969–11974.

89 Y. Kanemitsu, Halide perovskite nanocrystals: unique luminescence materials, *J. Lumin.*, 2022, **251**, 119207.

90 Y. Kanemitsu, Photophysics of halide perovskite nanocrystal quantum dots, *Nano Res.*, 2024, **17**, 10536–10542.

91 Y. Louyer, L. Biadala, P. Tamarat and B. Lounis, Spectroscopy of neutral and charged exciton states in single CdSe/ZnS nanocrystals, *Appl. Phys. Lett.*, 2010, **96**, 203111.

92 H. Htoon, A. V. Malko, D. Bussian, J. Vela, Y. Chen, J. A. Hollingworth and V. I. Klimov, Highly Emissive Multiexcitons in Steady-State Photoluminescence of Individual "Giant" CdSe/CdS Core/Shell Nanocrystals, *Nano Lett.*, 2010, **10**, 2401–2407.

93 Y. Louyer, L. Biadala, J. B. Trebbia, M. J. Fernée, P. Tamarat and B. Lounis, Efficient Biexciton Emission in Elongated CdSe/ZnS Nanocrystals, *Nano Lett.*, 2011, **11**, 4370–4375.

94 S. A. Empedocles, D. J. Norris and M. G. Bawendi, Photoluminescence Spectroscopy of Single CdSe Nanocrystallite Quantum Dots, *Phys. Rev. Lett.*, 1996, **77**, 3873.

95 L. Biadala, Y. Louyer, P. Tamarat and B. Lounis, Direct Observation of the Two Lowest Exciton Zero-Phonon Lines in Single CdSe/ZnS Nanocrystals, *Phys. Rev. Lett.*, 2009, **103**, 037404.

96 B. A. Koscher, J. K. Swabeck, N. D. Bronstein and A. P. Alivisatos, Essentially Trap-Free $CsPbBr_3$ Colloidal Nanocrystals by Postsynthetic Thiocyanate Surface Treatment, *J. Am. Chem. Soc.*, 2017, **139**, 6566–6569.

97 N. Yarita, H. Tahara, M. Saruyama, T. Kawawaki, R. Sato, T. Teranishi and Y. Kanemitsu, Impact of Postsynthetic Surface Modification on Photoluminescence Intermittency in Formamidinium Lead Halide Perovskite Nanocrystals, *J. Phys. Chem. Lett.*, 2017, **8**, 6041–6047.

98 S. Nakahara, H. Tahara, G. Yumoto, T. Kawawaki, M. Saruyama, R. Sato, T. Teranishi and Y. Kanemitsu, Suppression of Trion Formation in $CsPbBr_3$ Perovskite Nanocrystals by Postsynthetic Surface Modification, *J. Phys. Chem. C*, 2018, **122**, 22188–22193.

99 P. C. Sercel, J. L. Lyons, N. Bernstein and A. L. Efros, Quasicubic model for metal halide perovskite nanocrystals, *J. Chem. Phys.*, 2019, **151**, 234106.

100 K. Galkowski, A. Mitioglu, A. Miyata, P. Plochocka, O. Portugall, G. E. Eperon, J. T.-W. Wang, T. Stergiopoulos, S. D. Stranks, H. J. Snaith and R. J. Nicholas, Determination of the exciton binding energy and effective masses for methylammonium and formamidinium lead tri-halide perovskite semiconductors, *Energy Environ. Sci.*, 2016, **9**, 962–970.

101 Z. Yang, A. Surrente, K. Galkowski, A. Miyata, O. Portugall, R. J. Sutton, A. A. Haghighirad, H. J. Snaith, D. K. Maude, P. Plochocka and R. J. Nicholas, Impact of the Halide Cage on the Electronic Properties of Fully Inorganic Cesium Lead Halide Perovskites, *ACS Energy Lett.*, 2017, **2**, 1621–1627.

102 Y. Yamada and Y. Kanemitsu, Electron-phonon interactions in halide perovskites, *NPG Asia Mater.*, 2022, **14**, 48.

103 M. Fu, P. Tamarat, H. Huang, J. Even, A. L. Rogach and B. Lounis, Neutral and Charged Exciton Fine Structures in Single Lead Halide Perovskite Nanocrystals Revealed by Magneto-optical Spectroscopy, *Nano Lett.*, 2017, **17**, 2895–2901.

104 J. Ramade, L. M. Andriambariarijaona, V. Steinmetz, N. Goubet, L. Legrand, T. Barisien, F. Bernardot, C. Testelin, E. Lhuillier, A. Bramati and M. Chamarro, Fine structure of excitons and electron–hole exchange energy in polymorphic $CsPbBr_3$ single nanocrystals, *Nanoscale*, 2018, **10**, 6393–6401.

105 C. Yin, L. Chen, N. Song, Y. Lv, F. Hu, C. Sun, W. W. Yu, C. Zhang, X. Wang, Y. Zhang and M. Xiao, Bright-exciton fine-structure splittings in single perovskite nanocrystals, *Phys. Rev. Lett.*, 2017, **119**, 026401.

106 P. Tamarat, M. I. Bodnarchuk, J.-B. Trebbia, R. Erni, M. V. Kovalenko, J. Even and B. Lounis, The ground exciton state of formamidinium lead bromide perovskite nanocrystals is a singlet dark state, *Nat. Mater.*, 2019, **18**, 717–724.

107 P. Tamarat, L. Hou, J.-B. Trebbia, A. Swarnkar, L. Biadala, Y. Louyer, M. I. Bodnarchuk, M. V. Kovalenko, J. Even and B. Lounis, The dark exciton ground state promotes photon-pair emission in individual perovskite nanocrystals, *Nat. Commun.*, 2020, **11**, 6001.

108 P. Tamarat, E. Prin, Y. Berezovska, A. Moskalenko, T. P. T. Nguyen, C. Xia, L. Hou, J.-B. Trebbia, M. Zacharias, L. Pedesseau, C. Katan, M. I. Bodnarchuk, M. V. Kovalenko, J. Even and B. Lounis, Universal scaling laws for charge-carrier interactions with quantum confinement in lead-halide perovskites, *Nat. Commun.*, 2023, **14**, 229.

109 P. C. Sercel, J. L. Lyons, D. Wickramaratne, R. Vaxenburg, N. Bernstein and A. L. Efros, Exciton Fine Structure in Perovskite Nanocrystals, *Nano Lett.*, 2019, **19**, 4068–4077.

110 D. Weinberg, Y. Park, D. T. Limmer and E. Rabani, Size-Dependent Lattice Symmetry Breaking Determines the

Exciton Fine Structure of Perovskite Nanocrystals, *Nano Lett.*, 2023, **23**, 4997–5003.

111 S. Liu, A. R. DeFilippo, M. Balasubramanian, Z. Liu, S. G. Wang, Y.-S. Chen, S. Chariton, V. Prakapenka, X. Luo, L. Zhao, J. S. Martin, Y. Lin, Y. Yan, S. K. Ghose and T. A. Tyson, High-Resolution *In situ* Synchrotron X-Ray Studies of Inorganic Perovskite $CsPbBr_3$: New Symmetry Assignments and Structural Phase Transitions, *Adv. Sci.*, 2021, **8**, 2003046.

112 M. W. Swift and J. L. Lyons, Lone-Pair Stereochemistry Induces Ferroelectric Distortion and the Rashba Effect in Inorganic Halide Perovskites, *Chem. Mater.*, 2023, **35**, 9370–9377.

113 R. D. Schaller and V. I. Klimov, High Efficiency Carrier Multiplication in PbSe Nanocrystals: Implications for Solar Energy Conversion, *Phys. Rev. Lett.*, 2004, **92**, 186601.

114 A. Ueda, K. Matsuda, T. Tayagaki and Y. Kanemitsu, Carrier multiplication in carbon nanotubes studied by femtosecond pump-probe spectroscopy, *Appl. Phys. Lett.*, 2008, **92**, 233105.

115 Y. Kanemitsu, Multiple Exciton Generation and Recombination in Carbon Nanotubes and Nanocrystals, *Acc. Chem. Res.*, 2013, **46**, 1358–1366.

116 V. I. Klimov, A. A. Mikhailovsky, S. Xu, A. Malko, J. A. Hollingsworth, C. A. Leatherdale, H.-J. Eisler and M. G. Bawendi, Optical Gain and Stimulated Emission in Nanocrystal Quantum Dots, *Science*, 2000, **290**, 314–317.

117 M. Nirmal, B. O. Dabbousi, M. G. Bawendi, J. J. Macklin, J. K. Trautman, T. D. Harris and L. E. Brus, Fluorescence intermittency in single cadmium selenide nanocrystals, *Nature*, 1996, **383**, 802–804.

118 A. L. Eflos and D. J. Nesbitt, Origin and control of blinking in quantum dots, *Nat. Nanotechnol.*, 2016, **11**, 661–671.

119 G. Nair, J. Zhao and M. G. Bawendi, Biexciton Quantum Yield of Single Semiconductor Nanocrystals from Photon Statistics, *Nano Lett.*, 2011, **11**, 1136–1140.

120 N. Hiroshige, T. Ihara and Y. Kanemitsu, Simultaneously measured photoluminescence lifetime and quantum yield of two-photon cascade emission on single CdSe/ZnS nanocrystals, *Phys. Rev. B*, 2017, **95**, 245307.

121 N. Hiroshige, T. Ihara, M. Saruyama, T. Teranishi and Y. Kanemitsu, Coulomb-Enhanced Radiative Recombination of Biexcitons in Single Giant-Shell CdSe/CdS Core/Shell Nanocrystals, *J. Phys. Chem. Lett.*, 2017, **8**, 1961–1966.

122 M. Li, R. Begum, J. Fu, Q. Xu, T. M. Koh, S. A. Veldhuis, M. Grätzel, N. Mathews, S. Mhaisalkar and T. C. Sum, Low threshold and efficient multiple exciton generation in halide perovskite nanocrystals, *Nat. Commun.*, 2018, **9**, 4197.

123 Y. Chen, J. Yin, Q. Wei, C. Wang, X. Wang, H. Ren, S. F. Yu, O. M. Bakr, O. F. Mohammed and M. Li, Multiple exciton generation in tin–lead halide perovskite nanocrystals for photocurrent quantum efficiency enhancement, *Nat. Photonics*, 2022, **16**, 485–490.

124 Y. Xu, Q. Chen, C. Zhang, R. Wang, H. Wu, X. Zhang, G. Xing, W. W. Yu, X. Wang, Y. Zhang and M. Xiao, Two-Photon-Pumped Perovskite Semiconductor Nanocrystal Lasers, *J. Am. Chem. Soc.*, 2016, **138**, 3761–3768.

125 G. Yumoto, H. Tahara, T. Kawawaki, M. Saruyama, R. Sato, T. Teranishi and Y. Kanemitsu, Hot Biexciton Effect on Optical Gain in $CsPbI_3$ Perovskite Nanocrystals, *J. Phys. Chem. Lett.*, 2018, **9**, 2222–2228.

126 Y. Wang, M. Zhi, Y.-Q. Chang, J.-P. Zhang and Y. Chan, Stable, Ultralow Threshold Amplified Spontaneous Emission from $CsPbBr_3$ Nanoparticles Exhibiting Trion Gain, *Nano Lett.*, 2018, **18**, 4976–4984.

127 W. Zhao, Z. Qin, C. Zhang, G. Wang, X. Huang, B. Li, X. Dai and M. Xiao, Optical Gain from Biexcitons in $CsPbBr_3$ Nanocrystals Revealed by Two-dimensional Electronic Spectroscopy, *J. Phys. Chem. Lett.*, 2019, **10**, 1251–1258.

128 E. Kobiyama, H. Tahara, R. Sato, M. Saruyama, T. Teranishi and Y. Kanemitsu, Reduction of Optical Gain Threshold in $CsPbI_3$ Nanocrystals Achieved by Generation of Asymmetric Hot-Biexcitons, *Nano Lett.*, 2020, **20**, 3905–3910.

129 Z. Qin, Q. Zhang, L. Chen, T. Yu, X. Wang and M. Xiao, Electrical Switching of Optical Gain in Perovskite Semiconductor Nanocrystals, *Nano Lett.*, 2021, **21**, 7831–7838.

130 C. Zhu, M. Marczak, L. Feld, S. C. Boehme, C. Bernasconi, A. Moskalenko, I. Cherniukh, D. Dirin, M. I. Bodnarchuk, M. V. Kovalenko and G. Rainò, Room-Temperature, Highly Pure Single-Photon Sources from All-Inorganic Lead Halide Perovskite Quantum Dots, *Nano Lett.*, 2022, **22**, 3751–3760.

131 H. Igarashi, M. Yamauchi and S. Masuo, Correlation between Single-Photon Emission and Size of Cesium Lead Bromide Perovskite Nanocrystals, *J. Phys. Chem. Lett.*, 2023, **14**, 2441–2447.

132 N. Yarita, T. Aharen, H. Tahara, M. Saruyama, T. Kawawaki, R. Sato, T. Teranishi and Y. Kanemitsu, Observation of positive and negative trions in organic-inorganic hybrid perovskite nanocrystals, *Phys. Rev. Mater.*, 2018, **2**, 116003.

133 N. Yarita, H. Tahara, T. Ihara, T. Kawawaki, R. Sato, M. Saruyama, T. Teranishi and Y. Kanemitsu, Dynamics of Charged Excitons and Biexcitons in $CsPbBr_3$ Perovskite Nanocrystals Revealed by Femtosecond Transient-Absorption and Single-Dot Luminescence Spectroscopy, *J. Phys. Chem. Lett.*, 2017, **8**, 1413–1418.

134 Y. Kanemitsu, Trion dynamics in lead halide perovskite nanocrystals, *J. Chem. Phys.*, 2019, **151**, 170902.

135 G. Yumoto and Y. Kanemitsu, Biexciton dynamics in halide perovskite nanocrystals, *Phys. Chem. Chem. Phys.*, 2022, **24**, 22405–22425.

136 R. Matsunaga, K. Matsuda and Y. Kanemitsu, Observation of Charged Excitons in Hole-Doped Carbon Nanotubes

Using Photoluminescence and Absorption Spectroscopy, *Phys. Rev. Lett.*, 2011, **106**, 037404.
137 Y. Masumoto, S. Okamoto and S. Katayanagi, Biexciton binding energy in CuCl quantum dots, *Phys. Rev. B*, 1994, **50**, 18658.
138 M. Achermann, J. A. Hollingsworth and V. I. Klimov, Multiexcitons confined within a subexcitonic volume: Spectroscopic and dynamical signatures of neutral and charged biexcitons in ultrasmall semiconductor nanocrystals, *Phys. Rev. B*, 2003, **68**, 245302.
139 T. P. T. Nguyen, S. A. Blundell and C. Guet, Calculation of the biexciton shift in nanocrystals of inorganic perovskites, *Phys. Rev. B*, 2020, **101**, 125424.
140 C. Zhu, T. Nguyen, S. C. Boehme, A. Moskalenko, D. N. Dirin, M. I. Bodnarchuk, C. Katan, J. Even, G. Rainò and M. V. Kovalenko, Many-Body Correlations and Exciton Complexes in $CsPbBr_3$ Quantum Dots, *Adv. Mater.*, 2023, **35**, 2208354.
141 Y. Park and D. T. Limmer, Biexcitons are bound in $CsPbBr_3$ perovskite nanocrystals, *Phys. Rev. Mater.*, 2023, **7**, 106002.
142 J. L. Movilla, J. Planelles and J. I. Climente, Binding energy of polaronic trions and biexcitons in $CsPbBr_3$ nanocrystals, *Phys. Rev. B*, 2025, **111**, 155304.
143 J. Planelles, J. I. Climente and J. L. Movilla, Internal dynamics and dielectric screening of confined multiexciton states, *Phys. Rev. B*, 2025, **112**, 115434.
144 Y. Kayanuma, Quantum-Size Effects of Interacting Electrons and Holes in Semiconductor Microcrystals with Spherical Shape, *Phys. Rev. B*, 1988, **38**, 9797.
145 T. Takagahara, Biexciton States in Semiconductor Quantum Dots and Their Nonlinear Optical Properties, *Phys. Rev. B*, 1989, **39**, 10206.
146 Y. Z. Hu, M. Lindberg and S. W. Koch, Theory of Optically Excited Intrinsic Semiconductor Quantum Dots, *Phys. Rev. B*, 1990, **42**, 1713.
147 T. Takagahara, Effect of Dielectric Confinement and Electron-Hole Exchange Interaction on Excitonic States in Semiconductor Quantum Dots, *Phys. Rev. B*, 1993, **47**, 45690.
148 R. Romestain and G. Fishman, Excitonic Wave Function, Correlation Energy, Exchange Energy, and Oscillator Strength in a Cubic Quantum Dots, *Phys. Rev. B*, 1994, **49**, 1774.
149 P. G. Bolcatto and C. R. Proetto, Shape and Dielectric Mismatch Effects in Semiconductor Quantum Dots, *Phys. Rev. B*, 1999, **59**, 12487.
150 M. Nagai, T. Tomioka, M. Ashida, M. Hoyano, R. Akashi, Y. Yamada, T. Aharen and Y. Kanemitsu, Longitudinal Optical Phonons Modified by Organic Molecular Cation Motions in Organic-Inorganic Hybrid Perovskites, *Phys. Rev. Lett.*, 2018, **121**, 145506.
151 M. R. Filip, J. B. Haber and J. B. Neaton, Phonon Screening of Excitons in Semiconductors: Halide Perovskites and Beyond, *Phys. Rev. Lett.*, 2021, **127**, 067401.
152 Y. Park and D. T. Limmer, Renormalization of excitonic properties by polar phonons, *J. Chem. Phys.*, 2022, **157**, 104116.
153 T. Handa, T. Yamada, M. Nagai and Y. Kanemitsu, Phonon, thermal, and thermo-optical properties of halide perovskites, *Phys. Chem. Chem. Phys.*, 2020, **22**, 26069–26087.
154 M. Sendner, P. K. Nayak, D. A. Egger, S. Beck, C. Müller, B. Epding, W. Kowalsky, L. Kronik, H. J. Snaith, A. Pucci and R. Lovrinčić, Optical phonons in methylammonium lead halide perovskites and implications for charge transport, *Mater. Horiz.*, 2016, **3**, 613–620.
155 K. Miyata, D. Meggiolaro, M. T. Trinh, P. P. Joshi, E. Mosconi, S. C. Jones, F. De Angelis and X.-Y. Zhu, Large polarons in lead halide perovskites, *Sci. Adv.*, 2017, **3**, e1701217.
156 Y. Yang, D. P. Ostrowski, R. M. France, K. Zhu, J. van de Lagemaat, J. M. Luther and M. C. Beard, Observation of a hot-phonon bottleneck in lead-iodide perovskites, *Nat. Photonics*, 2016, **10**, 53–59.
157 M. Li, J. Fu, Q. Xu and T. C. Sum, Slow-Hot-Carrier Cooling in Halide Perovskites: Prospects for Hot-Carrier Solar Cells, *Adv. Mater.*, 2019, **31**, 1802486.
158 S.-T. Ha, C. Shen, J. Zhang and Q. Xiong, Laser cooling of organic–inorganic lead halide perovskites, *Nat. Photonics*, 2016, **10**, 115–121.
159 T. Yamada, T. Aharen and Y. Kanemitsu, Up-converted photoluminescence from $CH_3NH_3PbI_3$ perovskite semiconductors: Implications for laser cooling, *Phys. Rev. Mater.*, 2019, **3**, 024601.
160 M. Li, S. Bhaumik, T. W. Goh, M. S. Kumar, N. Yantara, M. Grätzel, S. Mhaisalkar, N. Mathews and T. C. Sum, Slow cooling and highly efficient extraction of hot carriers in colloidal perovskite nanocrystals, *Nat. Commun.*, 2017, **8**, 14350.
161 J. Chen, M. E. Messing, K. Zheng and T. Pullerits, Cation-Dependent Hot Carrier Cooling in Halide Perovskite Nanocrystals, *J. Am. Chem. Soc.*, 2019, **141**, 3532–3540.
162 L. Dai, Z. Deng, F. Auras, H. Goodwin, Z. Zhang, J. C. Walmsley, P. D. Bristowe, F. Deschler and N. C. Greenham, Slow carrier relaxation in tin-based perovskite nanocrystals, *Nat. Photonics*, 2021, **15**, 696–702.
163 B. Yu, L. Chen, Z. Qu, C. Zhang, Z. Qin, X. Wang and M. Xiao, Size-Dependent Hot Carrier Dynamics in Perovskite Nanocrystals Revealed by Two-Dimensional Electronic Spectroscopy, *J. Phys. Chem. Lett.*, 2021, **12**, 238–244.
164 J. W. M. Lim, Y. Guo, M. Feng, R. Cai and T. C. Sum, Making and Breaking of Exciton Cooling Bottlenecks in Halide Perovskite Nanocrystals, *J. Am. Soc. Chem.*, 2024, **146**, 437–449.
165 M. Yurii, S. Zhang, M. C. Brennan, B. Janko and M. Kuno, Photoluminescence Up-Conversion in $CsPbBr_3$ Nanocrystals, *ACS Energy Lett.*, 2017, **2**, 2514–2515.
166 A. G. del Águila, T. T. H. Do, J. Xing, W. J. Jee, J. B. Khurgin and Q. Xiong, Efficient up-conversion photo-

luminescence in all-inorganic lead halide perovskite nanocrystals, *Nano Res.*, 2020, **13**, 1962–1969.

167 B. J. Roman, N. M. Villegas, K. Lytle and M. Sheldon, Optically Cooling Cesium Lead Tribromide Nanocrystals, *Nano Lett.*, 2020, **20**, 8874–8879.

168 Y. Kajino, S. Otake, T. Yamada, K. Kojima, T. Nakamura, A. Wakamiya, Y. Kanemitsu and Y. Yamada, Anti-Stokes photoluminescence from $CsPbBr_3$ nanostructures embedded in a Cs_4PbBr_6 crystal, *Phys. Rev. Mater.*, 2022, **6**, L043001.

169 Z. Zhang, S. Ghonge, Y. Ding, S. Zhang, M. Berciu, R. D. Schaller, B. Jankó and M. Kuno, Resonant Multiple-Phonon Absorption Causes Efficient Anti-Stokes Photoluminescence in $CsPbBr_3$ Nanocrystals, *ACS Nano*, 2024, **18**, 6438–6444.

170 Y. Yamada, T. Oki, T. Morita, T. Yamada, M. Fukuda, S. Ichikawa, K. Kojima and Y. Kanemitsu, Optical Cooling of Dot-in-Crystal Halide Perovskites: Challenges of Nonlinear Exciton Recombination, *Nano Lett.*, 2024, **24**, 11255–11261.

171 Y. Yamada and Y. Kanemitsu, Cooling Semiconductors with Light: The Role of Electron–Phonon Interactions and Nanostructures, *J. Phys. Chem. Lett.*, 2025, **16**, 4496–4504.

172 A. S. Abbas, B. C. Li, R. D. Schaller, V. B. Prakapenka, S. Chariton, D. Bian, G. S. Engel and A. P. Alivisatos, Efficient up-conversion in $CsPbBr_3$ Nanocrystals via phonon-driven exciton-polaron formation, *Nat. Commun.*, 2025, **16**, 5803.

173 H. Utzat, W. Sun, A. E. K. Kaplan, F. Krieg, M. Ginterseder, B. Spokoyny, N. D. Klein, K. E. Shulenberger, C. F. Perkinson, M. V. Kovalenko and M. G. Bawendi, Coherent single-photon emission from colloidal lead halide perovskite quantum dots, *Science*, 2019, **363**, 1068–1072.

174 Y. Lv, C. Yin, C. Zhang, W. W. Yu, X. Wang, Y. Zhang and M. Xiao, Quantum Interference in a Single Perovskite Nanocrystal, *Nano Lett.*, 2019, **19**, 4442–4447.

175 A. E. K. Kaplan, C. J. Krajewska, A. H. Proppe, W. Sun, T. Sverko, D. B. Berkinsky, H. Utzat and M. G. Bawendi, Hong–Ou–Mandel interference in colloidal $CsPbBr_3$ perovskite nanocrystals, *Nat. Photonics*, 2023, **17**, 775–780.

176 M. A. Pérez-Osorio, R. L. Milot, M. R. Filip, J. B. Patel, L. M. Herz, M. B. Johnston and F. Giustino, Vibrational Properties of the Organic–Inorganic Halide Perovskite $CH_3NH_3PbI_3$ from Theory and Experiment: Factor Group Analysis, First-Principles Calculations, and Low-Temperature Infrared Spectra, *J. Phys. Chem. C*, 2015, **119**, 25703–25718.

177 T. Tadano, Y. Gohda and S. Tsuneyuki, Anharmonic force constants extracted from first-principles molecular dynamics: applications to heat transfer simulations, *J. Phys.:Condens. Matter*, 2014, **26**, 225402.

178 A. C. Ferreira, S. Paofai, A. Létoublon, J. Ollivier, S. Raymond, B. Hehlen, B. Rufflé, S. Cordier, C. Katan, J. Even and P. Bourges, Direct evidence of weakly dispersed and strongly anharmonic optical phonons in hybrid perovskites, *Commun. Phys.*, 2020, **3**, 48.

179 S. Nomura and T. Kobayashi, Exciton–LO-phonon couplings in spherical semiconductor microcrystallites, *Phys. Rev. B*, 1992, **45**, 1305.

180 S. A. Empedocles and M. G. Bawendi, Quantum-Confined Stark Effect in Single CdSe Nanocrystallite Quantum Dots, *Science*, 1997, **278**, 2114–2117.

181 J. Cui, A. P. Beyler, I. Coropceanu, L. Cleary, T. R. Avila, Y. Chen, J. M. Cordero, S. L. Heathcote, D. K. Harris, O. Chen, J. Cao and M. G. Bawendi, Evolution of the Single-Nanocrystal Photoluminescence Linewidth with Size and Shell: Implications for Exciton–Phonon Coupling and the Optimization of Spectral Linewidths, *Nano Lett.*, 2016, **16**, 289–296.

182 D. K. Sharma, S. Hirata, V. Biju and M. Vacha, Stark Effect and Environment-Induced Modulation of Emission in Single Halide Perovskite Nanocrystals, *ACS Nano*, 2019, **13**, 624–632.

183 B. Lv, T. Zhu, Y. Tang, Y. Lv, C. Zhang, X. Wang, D. Shu and M. Xiao, Probing Permanent Dipole Moments and Removing Exciton Fine Structures in Single Perovskite Nanocrystals by an Electric Field, *Phys. Rev. Lett.*, 2021, **126**, 197403.

184 M. Shim and P. Guyot-Sionnest, Permanent dipole moment and charges in colloidal semiconductor quantum dots, *J. Chem. Phys.*, 1999, **111**, 6955–6964.

185 S.-J. Park, S. Link, W. L. Miller, A. Gesquiere and P. F. Barbara, Effect of electrical field on the photoluminescence intensity of single CdSe nanocrystals, *Chem. Phys.*, 2007, **341**, 169–174.

186 H. Ibuki, T. Ihara and Y. Kanemitsu, Spectral Diffusion of Emissions of Excitons and Trions in Single CdSe/ZnS Nanocrystals: Charge Fluctuations in and around Nanocrystals, *J. Phys. Chem. C*, 2016, **120**, 23772–23779.

187 N. Q. Huong and J. L. Birman, Origin of polarization in polar nanocrystals, *J. Chem. Phys.*, 1998, **108**, 1769–1772.

188 S. Chen, J. Wang, S. Thomas, W. J. Mir, B. Shao, J. Lu, Q. Wang, P. Gao, O. F. Mohammed, Y. Han and O. M. Bakr, Atomic-Scale Polarization and Strain at the Surface of Lead Halide Perovskite Nanocrystals, *Nano Lett.*, 2023, **23**, 6002–6009.

189 Q. Zhao, A. Hazarika, L. T. Schelhas, J. Liu, E. A. Gaulding, G. Li, M. Zhang, M. F. Toney, P. C. Sercel and J. M. Luther, Size-Dependent Lattice Structure and Confinement Properties in $CsPbI_3$ Perovskite Nanocrystals: Negative Surface Energy for Stabilization, *ACS Energy Lett.*, 2020, **5**, 238–247.

190 G. Rainò, N. Yazdani, S. C. Boehme, M. Kober-Czerny, C. Zhu, F. Krieg, M. D. Rossell, R. Erni, V. Wood, I. Infante and M. V. Kovalenko, Ultra-narrow room-temperature emission from single $CsPbBr_3$ perovskite quantum dots, *Nat. Commun.*, 2022, **13**, 2587.

191 S. Hirotsu, J. Harada, M. Iizumi and K. Gesi, Structural Phase Transitions in $CsPbBr_3$, *J. Phys. Soc. Jpn.*, 1974, **37**, 1393–1398.

192 A. Poglitsch and D. Weber, Dynamic disorder in methylammoniumtrihalogenoplumbates (II) observed by millimeter-wave spectroscopy, *J. Chem. Phys.*, 1987, **87**, 6373–6378.

193 G. Mannino, I. Deretzis, E. Smecca, A. La Magna, A. Alberti, D. Ceratti and D. Cahen, Temperature-Dependent Optical Band Gap in $CsPbBr_3$, $MAPbBr_3$, and $FAPbBr_3$ Single Crystals, *J. Phys. Chem. Lett.*, 2020, **11**, 2490–2496.

194 A. D. Wright, C. Verdi, R. L. Milot, G. E. Eperon, M. A. Pérez-Osorio, H. J. Snaith, F. Giustino, M. B. Johnston and L. M. Herz, Electron–phonon coupling in hybrid lead halide perovskites, *Nat. Commun.*, 2016, **7**, 11755.

195 L. Q. Phuong, Y. Nakaike, A. Wakamiya and Y. Kanemitsu, Free Excitons and Exciton–Phonon Coupling in $CH_3NH_3PbI_3$ Single Crystals Revealed by Photocurrent and Photoluminescence Measurements at Low Temperatures, *J. Phys. Chem. Lett.*, 2016, **7**, 4905–4910.

196 J. Ramade, L. M. Andriambariarijaona, V. Steinmetz, N. Goubet, L. Legrand, T. Barisien, F. Bernardot, C. Testelin, E. Lhuillier, A. Bramati and M. Chamarro, Exciton-phonon coupling in a $CsPbBr_3$ single nanocrystal, *Appl. Phys. Lett.*, 2018, **112**, 072104.

197 M. Fu, P. Tamarat, J.-B. Trebbia, M. I. Bodnarchuk, M. V. Kovalenko, J. Even and B. Lounis, Unraveling exciton–phonon coupling in individual $FAPbI_3$ nanocrystals emitting near-infrared single photons, *Nat. Commun.*, 2018, **9**, 3318.

198 O. Pfingsten, J. Klein, L. Protesescu, M. I. Bodnarchuk, M. V. Kovalenko and G. Bacher, Phonon Interaction and Phase Transition in Single Formamidinium Lead Bromide Quantum Dots, *Nano Lett.*, 2018, **18**, 4440–4446.

199 S. Masada, T. Yamada, H. Tahara, H. Hirori, M. Saruyama, T. Kawawaki, R. Sato, T. Teranishi and Y. Kanemitsu, Effect of A-Site Cation on Photoluminescence Spectra of Single Lead Bromide Perovskite Nanocrystals, *Nano Lett.*, 2020, **20**, 4022–4028.

200 S. Rudin, T. L. Reinecke and B. Segall, Temperature-dependent exciton linewidths in semiconductors, *Phys. Rev. B*, 1990, **42**, 11218.

201 T. Yamada, T. Handa, Y. Yamada and Y. Kanemitsu, Light emission from halide perovskite semiconductors: bulk crystals, thin films, and nanocrystals, *J. Phys. D: Appl. Phys.*, 2021, **54**, 383011.

202 A. Alaei, A. Circelli, Y. Yuan, Y. Yang and S. S. Lee, Polymorphism in metal halide perovskites, *Mater. Adv.*, 2021, **2**, 47–63.

203 A. N. Goldstein, C. M. Echer and A. P. Alivisatos, Melting in semiconductor nanocrystals, *Science*, 1992, **256**, 1425–1427.

204 S. H. Tolbert and A. P. Alivisatos, Size dependence of a first order solid-solid phase transition: the wurtzite to rock salt transformation in CdSe nanocrystals, *Science*, 1994, **265**, 373–376.

205 P. Cottingham and R. L. Brutchey, Depressed Phase Transitions and Thermally Persistent Local Distortions in $CsPbBr_3$ Quantum Dots, *Chem. Mater.*, 2018, **30**, 6711–6716.

206 M. C. Brennan, M. Kuno and S. Rouvimov, Crystal Structure of Individual $CsPbBr_3$ Perovskite Nanocubes, *Inorg. Chem.*, 2019, **58**, 1555–1560.

207 H. Lu, Z. V. Vardeny and M. C. Beard, Control of light, spin and charge with chiral metal halide semiconductors, *Nat. Rev. Chem.*, 2022, **6**, 470–485.

208 C. B. Murray, C. R. Kagan and M. G. Bawendi, Self-Organization of CdSe Nanocrystallites into Three-Dimensional Quantum Dot Superlattices, *Science*, 1995, **270**, 1335–1338.

209 K. Hosoki, T. Tayagaki, S. Yamamoto, K. Matsuda and Y. Kanemitsu, Direct and Stepwise Energy Transfer from Excitons to Plasmons in Close-Packed Metal and Semiconductor Nanoparticle Monolayer Films, *Phys. Rev. Lett.*, 2008, **100**, 207404.

210 O. E. Semonin, J. M. Luther, S. Choi, H. Y. Chen, J. Gao, A. J. Nozik and M. C. Beard, Peak External Photocurrent Quantum Efficiency Exceeding 100% via MEG in a Quantum Dot Solar Cell, *Science*, 2011, **334**, 1530–1533.

211 M. Ono, T. Nishihara, T. Ihara, M. Kikuchi, A. Tanaka, M. Suzuki and Y. Kanemitsu, Impact of surface ligands on the photocurrent enhancement due to multiple exciton generation in close-packed nanocrystal thin films, *Chem. Sci.*, 2014, **5**, 2696–2701.

212 H. Tahara, M. Sakamoto, T. Teranishi and Y. Kanemitsu, Coherent electronic coupling in quantum dot solids induces cooperative enhancement of nonlinear opto-electronic responses, *Nat. Nanotechnol.*, 2024, **19**, 744–750.

213 G. Rainò, M. A. Becker, M. I. Bodnarchuk, R. F. Mahrt, M. V. Kovalenko and T. Stöferle, Superfluorescence from lead halide perovskite quantum dot superlattices, *Nature*, 2018, **563**, 671–675.

214 I. Cherniukh, G. Rainò, T. Stöferle, M. Burian, A. Travesset, D. Naumenko, H. Amenitsch, R. Erni, R. F. Mahrt, M. I. Bodnarchuk and M. V. Kovalenko, Perovskite-type superlattices from lead halide perovskite nanocubes, *Nature*, 2021, **593**, 535–542.